2

An Overview of Aerosol-Cloud Interactions

Hamish Gordon[1], Franziska Glassmeier[2], and Daniel T. McCoy[3]

ABSTRACT

Aerosol-cloud interactions refer to the group of atmospheric processes by which aerosols influence cloud properties, and sometimes also processes by which clouds affect aerosols. The effect of these atmospheric processes on Earth's radiative balance is potentially large, but uncertain. When combined with uncertainties in aerosol concentrations that result from emissions and aerosol processes, the uncertainty in aerosol-cloud interactions dominates the overall uncertainty in our knowledge of radiative forcing of Earth's climate. Aerosols affect clouds primarily by changing the number of cloud condensation and ice nuclei, "indirect effects," and sometimes also the temperature of the cloud, "semi-direct effects." Changes in cloud processes in response to aerosol-cloud interactions may cause significant adjustments to cloud macrophysical properties such as coverage and condensate amount. Aerosol-cloud interaction research focuses on understanding the atmospheric processes at work, mainly by analyzing observation data, performing laboratory experiments, and building models to simulate how aerosols influence clouds. In this review, we outline the relevant atmospheric science and highlight some promising techniques that have been applied recently to better understand aerosol-cloud interactions and their implications for radiative balance, such as Gaussian process emulation. This chapter is intended to provide background to subsequent chapters in this series of monographs and as an introduction for graduate students to current research in the field of aerosol-cloud interactions.

2.1. INTRODUCTION AND MOTIVATION

Aerosols are of fundamental importance to clouds. Without aerosols, relative humidities must reach 420% before condensation of water vapor will occur on ions, the next suitable surface in the atmosphere (Mason, 1960; Wilson 1900). Such high saturation ratios would be unlikely to occur near Earth's surface, as water would instead condense as dew, and so without aerosols, fogs and boundary-layer clouds would presumably be rare or absent. Conversely, in a world without clouds, atmospheric aerosols would also look very different, presumably existing in substantially higher concentrations.

[1]*Department of Chemical Engineering and Center for Atmospheric Particle Studies, Carnegie Mellon University, Pittsburgh, PA, USA*

[2]*Department of Geoscience and Remote Sensing, Delft University of Technology, Delft, The Netherlands*

[3]*Department of Atmospheric Science, University of Wyoming, Laramie, WY, USA*

2.1.1. The Importance of Aerosol-Cloud Interactions for Climate

The relevant question for climate, however, is how much difference to clouds is made by perturbations to a natural background level of aerosols. Changing the number of aerosols capable of acting as nuclei for water vapor to condense upon (cloud condensation nuclei, or CCN) leads to a change to the cloud droplet concentration, which in turn changes the reflectivity or albedo of

Clouds and Their Climatic Impacts: Radiation, Circulation, and Precipitation, Geophysical Monograph 281, First Edition.
Edited by Sylvia C. Sullivan and Corinna Hoose.

DOI: 10.1002/9781119700357.ch02

clouds. When kept separate from any change to the cloud condensate (liquid or ice mixing ratio) resulting from changing aerosol concentrations, this effect on cloud albedo is referred to as the Twomey effect (Twomey, 1974, 1977). In addition to the albedo, perturbations to cloud droplet concentrations also perturb microscopic processes inside clouds. These include collision-coalescence leading to the formation of warm rain (the Albrecht effect (Albrecht, 1989)), the condensation of supersaturated water vapor, the rate of sedimentation of cloud droplets, and the time needed for any given cloud droplet to evaporate. Changing the number of aerosols capable of acting as ice nuclei, the surfaces on which water can freeze, similarly influences the radiative properties of clouds and the probability of precipitation. Together, all of these processes by which aerosols affect cloud albedo and microphysical properties are known as indirect effects of aerosols on Earth's radiative balance. This distinguishes these aerosol effects from the "direct" effects of aerosols on radiation due to scattering and absorption, and from the thermodynamical perturbations to nearby clouds that result from aerosol absorption, termed semi-direct effects by Hanse et al. (1997).

The most obvious consequence of aerosol-cloud interactions, hereafter abbreviated as ACIs, for long-term radiation balance is apparent when the natural background level of aerosols is considered to be the pre-industrial atmosphere, and the perturbation is the total anthropogenic change in aerosol since pre-industrial times. Anthropogenic aerosols have led to an increase in the amount of radiation reflected by the Earth that has offset between 20% and 50% of the warming due to increased carbon dioxide concentrations over the industrial period (Bellouin et al., 2020; Charlson et al., 1992; Twomey, et al., 1984). The majority of this aerosol effect is due to the "indirect forcing of climate" by aerosols via ACIs, rather than due to the direct radiative effects of the aerosols themselves. The radiative forcing of Earth's climate due to the strengthening of the Twomey effect over time is usually abbreviated as RF_{aci}. When changes in cloud microphysical properties driven by aerosol, leading to *adjustments* in cloud macrophysical properties (e.g., area, thickness), are included, the resulting radiative forcing is termed an "effective" radiative forcing (ERF_{aci}). The large uncertainty in ERF_{aci}, which was estimated by Bellouin et al. (2020) to lie between -1.73 and $-0.27\ \mathrm{Wm}^{-2}$ (16–84% range), is the main motivation for the sustained efforts by the atmospheric community to better understand ACIs. Hansen et al. (2011) are more blunt, remarking that "Aerosol uncertainty is the principal barrier to quantitative understanding of on-going climate change". Thus, ACIs are critical to a treatment of the role of clouds in the climate system.

ACIs have numerous other more subtle implications for climate, as they are involved in several important feedback loops (Gettelman et al., 2016) and effects on atmospheric circulation (e.g., Mann et al., 2018; Wilcox et al. 2020). It is likely that changes in cloud cover and thickness in response to a warming atmosphere will be affected by changing aerosol concentrations as the climate warms, and, in turn, ERF_{aci} will be strongly affected by changing clouds in a future climate.

2.1.2. Outline and Aims of this Review

ACIs have been the subject of numerous recent review articles (Bellouin et al., 2020; Fan et al., 2016; Kreidenweis et al., 2019; Mülmenstädt et al., 2018; Rosenfeld et al., 2014· Seinfeld et al., 2016; Storelvmo, 2017; Tao et al., 2012) and we are aware of others in preparation. This contribution is selective rather than comprehensive and is intended to complement these alternative perspectives. We provide a brief introductory overview intended to provide context for later chapters in this monograph, followed by a characterization of some emerging trends in current research. We begin with a brief overview of the ACIs of interest in different meteorological regimes. We then discuss some key warm-cloud processes in detail: activation of aerosols, rain formation processes, and albedo. We follow with an overview of some new methodological approaches to disentangling ACIs. This is followed by discussion of cold clouds, and finally field experiments and satellite observations. To keep our review to a reasonable length, we do not discuss how clouds affect aerosols, although we do acknowledge that such effects may also have feedbacks to, and implications for, Earth's climate, as discussed by Carslaw et al. (2010) and Tegen and Schepanski (2018).

2.2. HOW AEROSOLS AFFECT DIFFERENT CLOUD TYPES

ACIs vary widely depending on the meteorological regime in which they occur. Some of the different regimes are illustrated in Figure 2.1.

Warm clouds are those which contain no ice and in which the temperature does not extend below 0°C; we note that supercooled liquid clouds are not warm. In warm non-raining low clouds (stratus and stratocumulus) and fogs found in the subtropics and midlatitudes, the size of the droplets for a given liquid water content (LWC) depends on the droplet number concentration. This dependence in turn leads to a significant and relatively well-understood effect of increasing droplet concentration on cloud albedo (RF_{aci}). The other possible ACIs of interest are evaporation-entrainment and

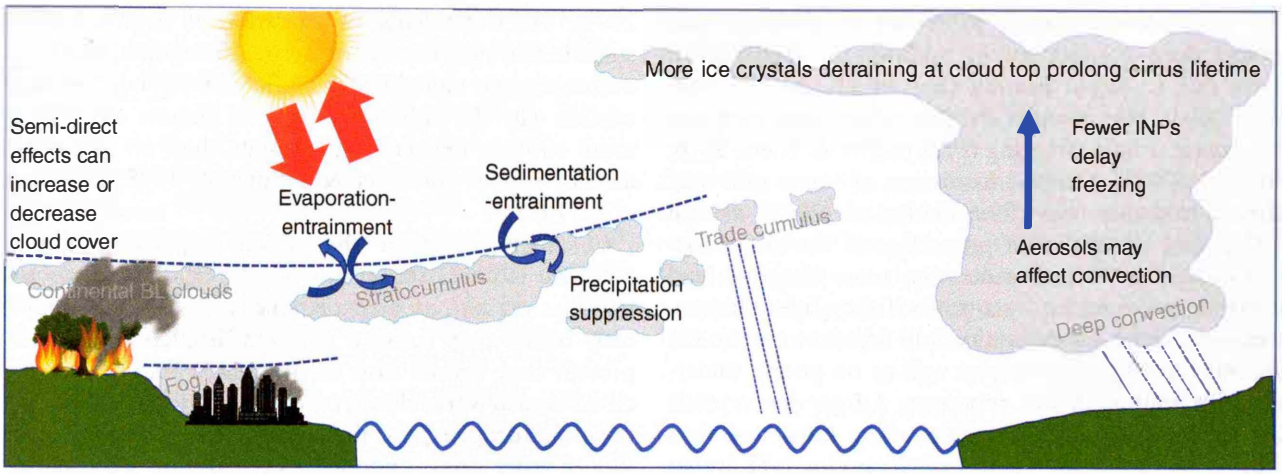

Figure 2.1 Schematic depicting some of the possible aerosol effects on clouds in the tropics and subtropics. Dashed lines denote temperature inversions.

sedimentation-entrainment feedbacks (Hill et al., 2009), which are also discussed in Chapter 12: Small-Scale Mixing of Clouds with Their Environment. Addressing sedimentation-entrainment feedbacks first, a higher droplet concentration leads to a slower sedimentation rate of droplets. Ackerman et al. (2004) showed that slower sedimentation will increase the entrainment of dry air into clouds, leading to more droplets evaporating, reducing the cloud albedo and water content. Bretherton et al. (2007) found that this increased entrainment was the result of more cloud water being concentrated at the top of the cloud when sedimentation is slower. As a result, evaporation rates at the cloud top are increased in proportion to the increased LWC, and entrainment is promoted by evaporative cooling. Furthermore, smaller droplets evaporate more quickly, promoting more turbulence and also increasing entrainment of dry air: the evaporation-entrainment feedback (Homann & Feingold, 2019; Small et al., 2009; Wang et al., 2003).

In warm raining clouds with low aerosol concentrations, a further ACI may become important: the Albrecht effect (Albrecht, 1989). This aerosol and precipitation regime is found frequently in the remote marine atmosphere. Recent research suggests the Albrecht effect is most important in very clean clouds, perhaps even only in clouds where the droplet concentration is below around 30 cm^{-3}, although this threshold is very uncertain. When aerosol concentrations are this low, droplets are large, and so fewer collision-coalescence events must take place to grow a cloud droplet into a drizzle or rain drop. Conversely, drizzle is suppressed in polluted conditions. Evidence stems from large eddy simulations and correlations in observations (e.g., Dagan al., 2015; Gryspeerdt, Goren, et al., 2019; Khairoutdinov & Kogan, 2000; Mann et al., 2014). The same mechanism may be active in slowing down precipitation processes at much higher droplet concentrations, for example in orographic clouds (Givati & Rosenfeld, 2004). However, some droplets nucleated on very large soluble aerosols, known as giant cloud condensation nuclei, grow efficiently into raindrops (Johnson, 1982) due to their high solute concentrations (Jensen & Nugent, 2017). Increasing concentrations of these large aerosols should, up to a point, hasten precipitation onset and reduce cloud liquid water paths (LWP) (Posselt & Lohmann, 2008).

Tropical trade cumulus, the topic of Chapter 7: Tropical Marine Low Clouds, and also congestus and deep convective clouds tend to have higher vertical velocities (greater than 1.0 ms^{-1}). In these clouds, concentrations of large aerosols are generally low (below 200 cm^{-3} in the accumulation mode), as these aerosols are often depleted by rainfall. Therefore, when compared to other cloud types, supersaturations may reach higher values, and smaller aerosols may be activated as droplets. Several authors have explored possible links between aerosol concentrations and the magnitude and altitude of latent heat release during condensation and freezing in clouds, and, by extension, if aerosols can influence how much condensation occurs in liquid and how much in ice phases of deep clouds. The effect of aerosols on deep clouds is discussed further in section 2.7. In brief, in more polluted clouds, in theory the larger surface area of aerosols should lead to more condensation at lower altitudes than in cleaner clouds. The lower altitude of the condensation and resultant latent heat release in more polluted clouds can affect updraft speeds but there is a lack of consensus in the community on the strength of these latent heating effects (Fan et al., 2007; Grabowski & Morrison, 2016, 2020).

In mixed-phase clouds, as found in cyclones and tropical deep convection, in addition to invigoration effects due to latent heating (Fan et al., 2018; Khain et al., 2004), high droplet concentrations may suppress or promote droplet freezing (Pruppacher & Klett, 2010; Yin et al., 2005). Delayed formation of warm rain may enhance cold rain later (Rosenfeld et al., 2008), as well as changing the radiative properties of the cloud top. If droplets freeze homogeneously, more droplets lead directly to more ice crystals, while if they freeze heterogeneously the ice concentration will depend more on the concentration of ice nuclei, as well as on poorly understood ice multiplication processes. Larger ice crystals have substantially higher sedimentation rates, and thus aerosols also affect the lifetime of cirrus clouds (Kärcher & Lohmann, 2003) and the mixed-phase clouds found at high latitudes.

2.3. AEROSOL ACTIVATION

With the exception of the semi-direct effect, all ACIs depend on the influence of aerosols on cloud droplet concentration. The major source of liquid droplet concentration in all warm clouds, and probably most cold clouds, is aerosol activation, and the source rate is determined by the cooling rate (usually the result of upward air motion), by the aerosol concentration and properties, and by the temperature. Sinks are droplet evaporation, droplet freezing, warm rain formation, and riming. Bellouin et al. (2020) estimate that cloud droplet concentrations increased by between 5% and 17% from 1850 to the period 2005–2015.

The activation of an aerosol particle to a cloud droplet occurs when the supersaturation of water vapor exceeds the critical supersaturation for that particle S_c. The supersaturation is generally the result of an air parcel cooling as it rises. S_c is given by

$$S_c = \left(\frac{4A^3}{27\kappa r_d^3} \right)^{1/2} \tag{2.1}$$

where A is proportional to the ratio of surface tension to temperature, κ is the volume-weighted hygroscopicity, and r_d is the dry radius of the aerosol (Ghan et al., 2011). Thus, for a given aerosol particle, the critical supersaturation depends principally on its size (Dusek et al., 2006) but also on hygroscopicity (Köhler, 1936; Petters & Kreidenweis, 2007) and surface tension (Prisle et al., 2012; Shulman et al., 1996). Larger, more hygroscopic particles with lower surface tension activate at lower supersaturations than smaller, less hygroscopic particles with higher surface tensions, and surface-bulk partitioning of molecules, especially surfactants, is also important in determining surface tension and hygroscopicity (Petters & Kreidenweis, 2013; Sullivan et al., 2009). The dependence of activation on hygroscopicity, sulfuric acid's key role in new aerosol formation, and large anthropogenic emissions of sulfur compounds together explain why the radiative forcing of climate by ACIs is more strongly dependent on sulfate than on any other aerosol species (Boucher & Lohmann, 1995; Charlson et al. 1992).

Calculating whether the critical supersaturation is exceeded requires accounting for the number of aerosol particles present, as aerosols take up water hygroscopically before they activate. If cloud droplets are already present they should also be accounted for. Well above cloud base in warm clouds (where activation is less likely), the cloud droplets, not the aerosols, likely dominate the sink of water vapor, and the supersaturation S is given by

$$S = \frac{w}{2\pi G} \frac{dq_l}{dz} \left(\frac{1}{N_d^2 q_l} \right)^{1/3} \tag{2.2}$$

where w is the vertical air velocity, G is a growth factor whose most important dependence is on temperature, q_l is LWC, z is height, and N_d is droplet concentration (Yang et al., 2019). A similar equation (Korolev & Mazin, 2003; Politovich & Cooper, 1988; Squires, 1952) does not require knowledge of $\frac{dq_l}{dz}$, but relies on the assumption of quasi steady state between the source of supersaturation, the updraft, and the sink of water vapor to droplets. This may be a good approximation even at the base of the cloud, provided turbulent fluctuations in vertical velocity are correctly accounted for (Prabhakaran et al. 2020). However, more complicated parameterizations accounting for the sink of water vapor to aerosols are usually used at cloud base (Ghan et al., 2011; Twomey, 1959); he most commonly used is that of Abdul-Razzak and Ghan (2000) which adopts the framework of Köhler (1936). More detailed models, often with bin-resolved cloud microphysics, are able to treat activation without the 'saturation adjustment' approximation that is typically used in weather and climate models (Khain et al., 2000). This approximation is the assumption that water vapor condenses on droplets or ice crystals sufficiently quickly that supersaturation is reduced to zero at the end of each model time step, at which point water vapor and condensate are in equilibrium. Detailed models without this assumption must treat supersaturation "prognostically," which means they must keep track of how it evolves from one time step to the next. These models are especially needed when activation within existing clouds is important (Fridlind et al. 2004), and potentially also fogs (Schwenkel & Maronga, 2019; Thouron et al., 2012). In fogs, supersaturation may be generated by radiative cooling, not by updraft velocities. Recently, however, approaches have been developed that will enable activation in fog or activation above cloud base to be

approximated to some extent in larger scale weather and climate models (Gordon et al., 2020; Poku et al., 2021; Wang et al., 2013; Yang et al., 2015).

Both aerosol size distributions (Kulkarni & Wang, 2006; Liu et al., 1974; Wang & Flagan, 1989) and CCN conce trations at different vapor supersaturations (Chuang et al., 2000; Hudson & Squires, 1976) can be measured accurately by in situ instrumentation aboard aircraft, as can cloud droplet size distributions (Baumgardner et al., 2001; Knollenberg, 1976) and updraft speeds (Axford, 1968; Wood et al., 1997). However, a perfect closure study of aerosol activation in the real atmosphere is elusive, mainly because droplets are not generally nucleated in the same place or at the same time as they are detected. Activation can be better observed in chamber experiments such as the Michigan Technological University Pi chamber (Prabhakaran et al., 2020; Shaw et al., 2020). This technology for cloud physics studies has stood the test of time (Aitken, 1881) and still offers great promise for ever more quantitative studies of the critical interactions between turbulence and microphysics.

2.4. WARM CLOUD ALBEDO

In the preceding section, we described the activation of aerosol into cloud droplets. Here, we describe how the ability of aerosol to control cloud droplet number concentration (N_d) allows aerosol to directly affect cloud albedo (α). Alteration in cloud albedo by aerosol through changing the number concentration of cloud droplets, separately to any changes to the cloud condensate amount, is known as the first indirect effect or Twomey effect (Twomey, 1977).

Based on Lorenz-Mie theory, the optical depth (τ) of a cloud is the extinction cross-section of a collection of liquid droplets with geometric radii (r) and size distribution of cloud droplets ($n_d(r)$)

$$\tau = \int_{z=0}^{h} \int_{0}^{\infty} Q_e \pi r^2 n_d(r) dr dz \tag{2.3}$$

where Q_e is the efficiency of extinction, z is vertical distance and h is the geometric cloud height, and $Q_e \approx 2$ for liquid cloud droplets. The effective radius (r_e) proportional to scattering area, is

$$r_e = \frac{\int_0^{\infty} r \cdot \pi r^2 n_d(r) dr}{\int_0^{\infty} \pi r^2 n_d(r) dr} \tag{2.4}$$

and LWC within some volume through the cloud is

$$LWC = \frac{4\pi}{3} \rho_{liq} \int_0^{\infty} r^3 n_d(r) dr \tag{2.5}$$

Dividing equation (2.5) by the integrand of the integral with respect to z in equation (2.3), assuming $Q_e \sim 2$, rearranging, and integrating with respect to height yields in terms of τ

$$\tau = \int_{z=0}^{h} \frac{3}{2\rho_{liq}} LWC(z)/r_e(z) dz \tag{2.6}$$

Following the original presentation of S. Twomey (1977), we wish to represent this in terms of the number concentration of cloud droplets N_d. This is useful because N_d depends mainly on the number concentration of CCN, and unlike r_e is to a first approximation independent of LWC. N_d is the LWC divided by droplet mass

$$N_d(z) = LWC(z) \cdot \left(\rho_{liq} \frac{4\pi r(z)^3}{3} \right)^{-1} \tag{2.7}$$

To calculate N_d from satellite data, a constant factor $k = r^3/r_e^3$ is inserted to allow the effective radius rather than the true radius to be used in this equation. An important feature of real clouds that must also be taken into account when measuring N_d from space is the degree to which they are subadiabatic (f_{ad}). We may represent the LWC of a cloud as a function of adiabaticity and cloud vertical extent

$$LWC(z) = f_{ad} \Gamma_{ad} z \tag{2.8}$$

where Γ_{ad} is the adiabatic rate of increase of LWC with height, a function of pressure and temperature. Using equations (2.8) and (2.7) in equation (2.6) we may write cloud optical depth as a function of N_d, cloud geometric depth and adiabaticity

$$\tau = A \cdot (f_{ad} \Gamma_{ad})^{2/3} N_d^{1/3} h^{5/3} \tag{2.9}$$

where A is a constant equal to $(243\pi/250\rho_{liq}^2)^{1/3}$. Thus, cloud optical depth is a weak function of N_d. This may also be written in terms of LWP instead of cloud thickness using the integrated version of equation (2.8)

$$\tau = N_d^{1/3} \cdot LWP^{5/6} \cdot A \cdot \left(\frac{32}{f_{ad} \Gamma_{ad}} \right)^{1/6} \tag{2.10}$$

Increasing N_d increases cloud optical depth and yields the first indirect effect or aerosol-cloud radiative effect. The dependence of cloud albedo, or reflectance on N_d is further muted: assuming conservative scattering allows us to approximate (Lacis & Hansen, 1974)

$$\alpha \sim \frac{\tau}{\tau + \eta} \tag{2.11}$$

where η is a constant that varies depending on the value of the asymmetry parameter (usually given symbol g) and on assumptions in the derivation of the equation. The asymmetry parameter is the intensity-weighted average of the cosine of the scattering angle. For a typical g of 0.85, η ranges between 7 (Petty, 2006) and 13.3 (Tornow et al., 2020). An interesting feature of the

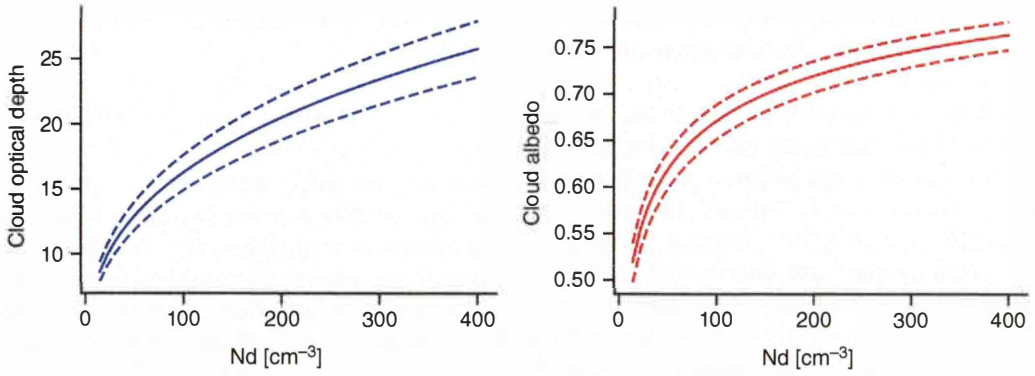

Figure 2.2 Cloud optical depth (τ) and albedo (α) as a function of N_d. Solid lines show a cloud with $LWP = 100\,\mathrm{g\,m^{-3}}$ and dashed lines show $LWP = 90\,\mathrm{g\,m^{-3}}$ and $110\,\mathrm{g\,m^{-3}}$. Cloud albedo is derived following the approximation in Lacis and Hansen (1974).

1/3 power to which N_d is raised and the relationship between α and τ is that at high N_d the effects of increasing N_d yield diminished returns. One consequence of this is the importance of the pre-industrial state in determining ERF_{aci} (Carslaw et al., 2013). The dependence of τ on N_d and α on τ is shown in Figure 2.2.

Aerosol-induced changes in cloud albedo translate into changes to the radiative balance at the top of the atmosphere R,

$$dR = d(R_{\mathrm{SW}}^{\mathrm{in}}[A_{\mathrm{cld}}c + (1-c)A_{\mathrm{clr}}] - R_{\mathrm{LW}}^{\mathrm{out}}) \tag{2.12}$$

where $R_{\mathrm{SW}}^{\mathrm{in}}$ denotes incoming shortwave radiation, $R_{\mathrm{LW}}^{\mathrm{out}}$ outgoing longwave radiation, c cloud fraction, and $A_{\mathrm{clr/cld}}$ the clear- and cloud-sky albedo at the top of the atmosphere. The longwave term in equation (2.12) can be neglected in warm clouds unless aerosol changes in cloud top temperature are of interest or the clouds are thin (e.g., Garrett et al., 1 February 2002). Furthermore, changes in $R_{\mathrm{SW}}^{\mathrm{in}}$ are usually also negligible, at least on sub-decadal timescales. Diamond et al. (2020) provide a recipe to relate changes in radiative balance to the albedo of a scene with partial cloud cover, accounting for the transmissivity and albedo of the atmosphere above clouds. Over ocean in unpolluted situations, when both the surface albedo and the albedo of the atmosphere above the clouds are small and the change in the cloud fraction is not too large, it may be possible to approximate equation (2.12) as

$$dR \propto d(\alpha \cdot c) \tag{2.13}$$

where α is the cloud albedo. However, over land or sea ice, in polluted conditions, and likely also for high or deep clouds (because the approximation relies on the above-cloud albedo being similar to the clear-sky albedo), equation (2.13) would not be valid.

2.5. APPROACHES TO DETERMINING SUSCEPTIBILITY

Aerosol effects on the radiative properties of clouds can be quantified by relating a change in scene albedo $dR = d(\alpha \cdot c)$ (equation (2.13)) to the perturbation in cloud droplet concentration dN_d that caused the change in scene albedo,

$$\frac{\mathrm{d}\ln R}{\mathrm{d}\ln N_d} = \frac{\mathrm{d}\ln \alpha}{\mathrm{d}\ln N_d} + \frac{\mathrm{d}\ln c}{\mathrm{d}\ln N_d}, \tag{2.14}$$

where the logarithmic derivative $\mathrm{d}\ln R/\mathrm{d}\ln N_d = (\mathrm{d}R/R)/(\mathrm{d}N_d/N_d)$ is introduced for convenience and will broadly be referred to as *susceptibility*, following Platnick and Twomey (1994). The perturbation in cloud droplet number concentration is assumed to be the result of a change in aerosol number concentration dN_a, not the result of precipitation or thermodynamic changes in the cloud. Its numerical value corresponds to the percentage change in R that is obtained for a 1% change in N_d. Expressing cloud albedo as a nested function of N_d,

$$\alpha = \alpha\{\tau[N_d, \mathrm{LWP}(N_d)]\}, \tag{2.15}$$

where $\alpha(\tau)$ is given by equation (2.11) and $\tau(N_d, \mathrm{LWP})$ by equation (2.10). Applying the chain rule provides the following simplification for warm clouds:

$$\begin{aligned}\frac{\mathrm{d}\ln \alpha}{\mathrm{d}\ln N_d} &= \frac{\partial \ln \alpha}{\partial \ln \tau}\frac{\mathrm{d}\ln \tau}{\mathrm{d}\ln N_d} \\ &= \frac{\partial \ln \alpha}{\partial \ln \tau}\left(\frac{\partial \ln \tau}{\partial \ln N_d} + \frac{\partial \ln \tau}{\partial \ln \mathrm{LWP}}\frac{\mathrm{d}\ln \mathrm{LWP}}{\mathrm{d}\ln N_d}\right) \\ &= (1-\alpha)\left(\frac{1}{3} + \frac{5}{6}\frac{\mathrm{d}\ln \mathrm{LWP}}{\mathrm{d}\ln N_d}\right)\end{aligned} \tag{2.16}$$

Note that partial derivatives (symbol: ∂) quantify changes that arise with respect to one specific variable, keeping all other variables at fixed values. Partial logarithmic derivatives of a power law like equation (2.10) correspond

to its exponents. They are thus independent of any constant pre-factors. Derivatives indicated by "d" comprise total changes, including nested dependencies. Such dependencies can encapsulate very complex relationships, for which no theoretical expressions are available; the LWP r sponse to droplet number perturbations, $\mathrm{d}\ln \mathrm{LWP}/\mathrm{d}\ln N_\mathrm{d}$, for example, depends on the full complexity of cloud dynamics.

Summarizing equations (2.14) and (2.16) yields the overall susceptibility of a partially cloudy scene (Bellouin et al., 2020),

$$\frac{\mathrm{d}\ln R}{\mathrm{d}\ln N_d} = \frac{1-\alpha}{3} + \frac{5(1-\alpha)}{6}\frac{\mathrm{d}\ln \mathrm{LWP}}{\mathrm{d}\ln N_d} + \frac{\mathrm{d}\ln c}{\mathrm{d}\ln N_d} \quad (2.17)$$

$$= \frac{\partial \ln R}{\partial \ln N_d} + \frac{\partial \ln R}{\partial \ln \mathrm{LWP}}\frac{\mathrm{d}\ln \mathrm{LWP}}{\mathrm{d}\ln N_d} + \frac{\partial \ln R}{\partial \ln c}\frac{\mathrm{d}\ln c}{\mathrm{d}\ln N_d} \quad (2.18)$$

where the first equality, like equation (2.16), strictly applies only to warm clouds. The second equality assumes that it is more generally suitable to quantify variability in R based on a functional relationship R=f(N_d, LWP, c). We can identify the first term on the right-hand side of equation (2.18) as a quantification of the Twomey effect, that is, the change of R with N_d, when keeping LWP (and c) constant. The second and third terms correspond to the response of LWP and c to changes in droplet number, respectively. These terms are usually referred to as LWP an cloud fraction *adjustments*.

Traditionally, logarithmic derivatives are empirically quantified as linear regression slopes in log-log space. Total derivatives correspond to one-dimensional linear regression (e.g., Quaas et al., 2009). For partial derivatives, other dependencies must be kept constant through stratification of the dataset (e.g., McComiskey et al., 2009), or controlled for by applying multi-linear regression (Fig. 2.3b).

The pragmatic linear regression approach faces methodological and conceptual difficulties. First of all, the linear regression approach only quantifies correlation but does not guarantee causality, that is, it is not clear if observed variability in LWP is indeed caused by variability in N_d (Gryspeerdt, Goren, et al., 2019; McCoy, Field, et al., 2020). As an example of a correlation between LWP and N_d that is not caused by cloud processes, consider a dataset that either samples under moist and clean oceanic conditions or under dry and polluted continental conditions. A second problem related to the regression approach is that the variability exhibited by a dataset varies with the *scale of data aggregation* (Bender et al., 2019; McComiskey & Feingold, 2012; Possner et al., 2016; Schutgens et al., 2016). Here, the scale of data aggregation refers to how data are averaged at a scale greater than the *process scale* at which ACI occurs before analysis is performed (McComiskey & Feingold, 2012).

A linear regression between the logarithms of quantities further assumes a power law relationship with constant exponents. It is thus not taken into account that such a relationship may only be a valid approximation under certain conditions. As an example, equation (2.10) is only valid if a broadening of the droplet size distribution from collision-coalescence can be neglected (Feingold et al., 1997). We consider LWP adjustments as another example of this challenge: Compare LWP adjustments in a raining and a non-raining warm cloud. For the raining state, we expect $\mathrm{d}\ln \mathrm{LWP}/\mathrm{d}\ln N_d > 0$ from rain suppression. For the non-raining state, droplet-size effects on entrainment dominate and $\mathrm{d}\ln \mathrm{LWP}/\mathrm{d}\ln N_d < 0$. In addition to this *state dependence*, which is tied to the internal state of a cloud field, the LWP adjustment may also depend on external cloud controlling factors, for example, on above-cloud moisture (Chen et al., 2014), which control the entrainment response to droplet size. We denote this as *regime dependence*. Both *state and regime dependence* of susceptibility can be accounted for by a stratification of the dataset prior to quantifying the aerosol-cloud relationship, in our example based on the occurrence of rain, and based on above-cloud moisture (Gryspeerdt, Goren, et al., 2019). Biases from imbalanced sampling within a specific state and regime, for example, in the form of sparsely sampled very high N_d in the non-precipitating regime for high above-cloud RH, can be addressed through joint histograms (e.g., Gryspeerdt, Goren, et al., 2019) or, equivalently, through the use of bin-average values (Glassmeier et al., 2021; Rosenfeld et al., 2019). Finally, the response dLWP to $\mathrm{d}N_d$ may not be instantaneous but evolve over time so that susceptibility is *time-dependent* on the time that has evolved since the aerosol conditions of a cloud system were perturbed (Glassmeier et al., 2021). The next section will discuss recent approaches to address these challenges.

2.6. NEW METHODOLOGICAL APPROACHES

The proliferation of new, increasingly sophisticated observations and new simulations with increasingly complex models and/or increasingly high grid resolution has led to an explosion in the availability of data that contains information on ACIs. To make sense of the data, new statistical approaches drawing on increasingly popular machine learning algorithms can be employed. We highlight here only a small sample of the techniques available, chosen according to our own familiarity with them.

2.6.1. Gaussian-Process Emulation to Address State Dependence

If the albedo susceptibility is not dependent on the state of the cloud field, in particular the absolute values of N_d, LWP, and c, the scene albedo R varies with cloud properties according to a power law, or log-log linear function,

$$R = i \cdot N_d^{\alpha} \mathrm{LWP}^{\beta} c^{\gamma} \Leftrightarrow \ln R = \ln i + \alpha \ln N_d + \beta \ln \mathrm{LWP} + \gamma \ln c, \quad (2.19)$$

where i, α, β, γ are constants that can be determined from multi-linear regression. Figure 2.3b illustrates a two-dimensional version of equation (2.19).

For a state-dependent susceptibility, scene albedo $R = f(N_d, \mathrm{LWP}, c)$ is given by a more complicated function f. Figure 2.3a illustrates such a functional relationship for our two-dimensional example. A power law approximation is possible for limited regions of the N_d-LWP state space, in particular for fully overcast states with $c \approx 1$. Beyond this region, the power law approximation cannot capture the full complexity of the R-state space relationship as indicated by the missing curvature of scene albedo isolines in Figure 2.3b. While a power law relationship can be determined from (log-log) linear regression, mapping-out relationships like the one illustrated in Figure 2.3a requires surrogate models, or emulators, for how R, or the complex function f, respectively, varies across state space. *Gaussian-process emulation* provides such a description. We refer the reader to Rasmussen and Williams (2006) and Lee et al. (2011) for a detailed explanation. The scene-albedo surface in Figure 2.3a corresponds to the mean of a two-dimensional Gaussian process (a functional analog of a multivariate Gaussian distribution), whose mean and covariance functions have been constrained by a set of training data points. This effectively corresponds to an interpolation between the known training data points with thoroughly quantified uncertainty (the latter is not illustrated in Fig. 2.3). Relationships obtained in this manner can then be differentiated to obtain state-dependent partial derivatives as illustrated in Figure 2.3c,d.

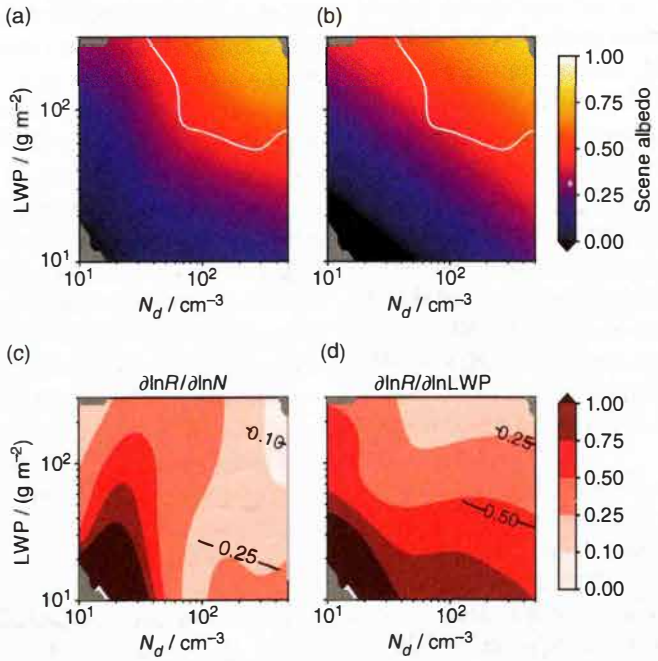

Figure 2.3 Scene albedo R' as a function of cloud droplet number concentration, N_d, and liquid-water path, LWP, as obtained from (a) Gaussian process emulation representing the general function $R' = f'(N_d, \mathrm{LWP}) = f[N_d, \mathrm{LWP}, c(N_d, \mathrm{LWP})]$ and (b) bi-linear regression with an underlying model $R' = \ln i' + \alpha' \ln N_d + \beta' \ln \mathrm{LWP}$ (cf. equation (2.19)). The white contour indicates where cloud fraction approaches unity, $c \approx 1$, such that fully overcast conditions are expected in the upper right corner of the N_d-LWP space. Comparing (a) and (b) in this region illustrates that the bi-linear model (b) is an appropriate approximation of the more complex relationship (a) under such conditions. (c, d) State-dependent values for partial derivatives (color contours) as derived from (a) and according to equation (2.17) (black line contours, only shown in the non-raining regime where they apply). Plots are adapted from Glassmeier et al. (2019) and apply to stratocumulus as modeled with large eddy simulations under the specific boundary conditions outlined in the reference.

2.6.2. Tendency Emulation to Address Time Dependence of Adjustments

Uncertainty in adjustments constitute an important uncertainty in overall ERF_{aci} (Bellouin et al., 2020). Forcing from adjustments in LWP was estimated to be between 0 and 0.56 Wm^{-2} and from adjustments in cloud cover to be between −1.14 and 0 Wm^{-2} (Bellouin et al., 2020) based on observational constraints. Thus, methods to leverage observations to constrain adjustments are impactful. LWP adjustments, $\text{adj} = d\ln \text{LWP}/d\ln N_d$, as well as cloud-fraction adjustments, $d\ln c/d\ln N_d$, aim to quantify the effect of perturbing certain cloud processes, like precipitation formation and entrainment, on the state of the cloud as captured by LWP and c. (A more direct, but also less feasible, way of doing so would be to quantify aerosol effects on process rates; see Mülmenstädt et al. (2020) for an interesting approach along these lines). These perturbations to process rates over time manifest in perturbations to the cloud state. In particular, they are absent at the moment of perturbation, $\text{adj}(t = 0) = 0$, where t indicates time since the perturbation. For stratocumulus cloud fraction, Christensen et al. (2020) show that initially strong aerosol effects arising from aerosol-enhanced cloud formation decrease over time. They specifically observe that differences in cloud fraction become less pronounced over a timescale of days. Also for stratocumulus, Glassmeier et al. (2021) have shown that the value of time-dependent adjustments, $\text{adj} = \text{adj}(t)$, evolves toward a steady state value $\text{adj}(\infty)$ according to

$$\text{adj}(t) = \text{adj}(\infty)\left[1 - \exp\left(-\frac{t}{\tau_{adj}}\right)\right], \tag{2.20}$$

where the equilibration timescale of the adjustment,

$$\tau_{\text{adj}} = \tau\left[1 - d \cdot \text{adj}(\infty)\right], \tag{2.21}$$

scales with the steady state value and $\tau = 9.6$ h and $d = 1.6$ are specific to the non-raining Sc studied. Glassmeier et al. (2021) determine the value of $\text{adj}(\infty)$ from short-term LWP tendencies, or LWP time series, respectively. Emulation of such tendencies $\nu = d\ln \text{LWP}/dt$ allows the authors to represent the LWP evolution of an Sc deck as a flow field $\nu(N_d, \text{LWP})$ in the space of Sc states spanned by N_d and LWP. Figure 2.4 illustrates such a flow field and its relationship to $\text{adj}(\infty)$.

2.6.3. Causality of LWP Adjustments

Examining covariances between aerosol, cloud microphysics (e.g., N_d), and cloud macrophysical quantities is inherently causally ambiguous. Covariances between these quantities can result from external factors as well as from real ACI (Stevens & Feingold, 2009), in contrast to the steady state adjustments discussed in section 2.6.2. In the case illustrated in Figure 2.5, N_d may affect LWC through adjustments (the strength of this effect is characterized as $d\ln LWP/d\ln N_d$, as discussed in section 2.5). Any change in liquid content may in turn affect precipitation processes in clouds that are precipitating or near to precipitating. However, precipitation strongly affects N_d through coalescence scavenging. Wood et al. (2012) estimate that precipitation scavenging reduces N_d by a factor of 2–3 over remote oceans. Precipitation also reduces concentrations of CCN by removing both interstitial and activated aerosol through wet scavenging. Air

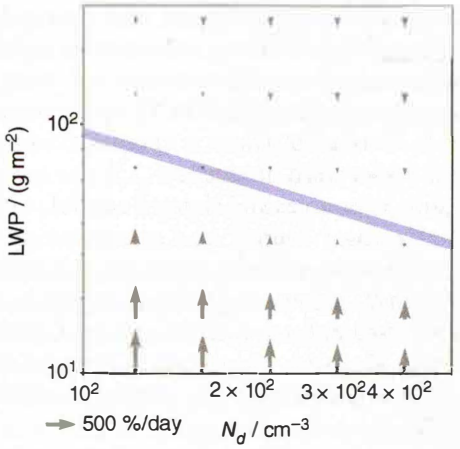

Figure 2.4 Liquid water path tendencies $\nu = d\ln \text{LWP}/dt$ as function of N_d and LWP. The LWP steady state, characterized by $\nu = 0$, is indicated by the blue line with negative slope (gray in monochrome version). Its slope corresponds to the steady state LWP adjustment $\text{adj}(\infty)$ defined in the text. See Glassmeier et al. (2021) for details.

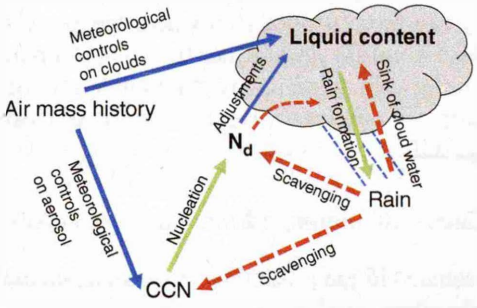

Figure 2.5 A schematic of causal links between cloud, aerosol, precipitation, and meteorology in warm clouds (Gryspeerdt, Goren, et al., 2019; McCoy, Field, et al., 2020; Michibata & Suzuki, 2020). Green lines (gray in monochrome version) indicate a positive relationship. Red (dashed in monochrome version) denotes a negative relationship. Blue (black in monochrome version) is ambiguous.

mass history affects both aerosol and clouds, inducing further potentially spurious covariance between N_d and cloud macrophysical properties and complicating the constraint of $d\ln LWP/d\ln N_d$ from observations (Mauger & Norris, 2007). As a specific example of the covariability discussed in section 2.5, the present-day configuration of sources and sinks of aerosol, with strong continental aerosol sources and strengthening precipitation away from continents, yields a spurious negative $d\ln LWP/d\ln N_d$ in important cloudy regions such as the stratocumulus-cumulus transition off the Chilean coast (Engstrom et al., 2015; Gryspeerdt, Goren, et al., 2019; Mauger & Norris, 2007; McCoy, Field et al., 2020; Wood et al., 2012).

Several methods have been proposed to cut this causal Gordian Knot. These must rely on either modeling (where causality can be controlled) or examining case studies where causality is mostly unambiguous (discussed below in section 2.6.4). An example of the empirical approach is given by Gryspeerdt, Goren, et al. (2019), who use variability observed by Moderate Resolution Imaging Spectroradiometer (MODIS) stratified according to volcanic emissions of aerosol to isolate a causal signal. Some examples of the modeling-based approach are given by D. T. McCoy et al. (2018) and McCoy, Field, et al. (2020), who utilize global simulations to study extratropical weather regimes where the effects of precipitation on aerosol and N_d are disabled to isolate the effect $N_d \rightarrow LWP$ and $N_d \rightarrow c$. The methodology assumes that models are able to replicate the effects of precipitation scavenging on N_d and CCN in a realistic manner and that nonlinear feedbacks between adjustments and precipitation are negligible (e.g., precipitation is primarily determined by the state of the atmosphere, not by adjustments).

In short, observational inference must either use a case study where causality is less opaque, or use a model where causality can be controlled (but where the model must be assumed to accurately reproduce the non-ACI parts of the system in Fig. 2.5) to infer $d\ln LWP/d\ln N_d$. In the following section, we will briefly discuss the use of case studies to study ACIs.

2.6.4. Causality Inference from Transient Events

As discussed in the preceding section, causal ambiguity greatly hampers our ability to cleanly infer the strength of ACIs from observations. Examination of case studies where changes in aerosol are disentangled from meteorology and precipitation has been used in many studies to constrain ACIs. These so-called *"opportunistic experiments"* in aerosol forcing offer an opportunity to assign causality to ACI inferred from observations (Christensen et al., 2021).

The canonical example of an opportunistic experiment is the bright lines left in cloud cover by ships (so-called ship tracks), which have been observed since the first satellite images of Earth (Conover, 1966). Ship tracks are a common feature of oceanic clouds in the anthropocene and many studies have examined their behavior in an attempt to isolate the effect of aerosol on clouds (Ackerman, Toon, Taylor, et al., 2000; Diamond et al., 2020; Goren & Rosenfeld, 2014; Gryspeerdt, Smith et al., 2019; Hobbs et al., 2000; Toll et al., 2017, 2019; Thornton et al., 2017) (Web of Science suggests >70 papers since 1990), although recent work shows that estimates of the radiative effect of ACI and LWP adjustments in Sc from ship tracks are up to 200% too large when compared to the climatological effect (Glassmeier et al., 2021).

While less visually striking, many other opportunistic experiments have been discovered and used to constrain ACI (M. Christensen et al., 2022). These include volcanic emissions of sulfur dioxide from strong emitters such as Kīlauea (Hawaii) (Fig. 2.6), Holuhraun (Iceland), and the Vanuatu archipelago (Carn et al., 2017; McCoy & Hartmann, 2015; Mace & Abernathy, 2016; McCoy et al., 2018; Malavelle et al., 2019; Yuan et al., 2011) as well as smaller sources such as the volcanoes on the Aleutian and Sandwich islands (Gassó, 2008). Volcanoes have the capability to substantially affect boundary layer aerosol and by extension cloud over duration of the eruption. However, this relatively short time period means that meteorological variability may make changes in cloud properties difficult to interpret (McCoy et al., 2018). Steady changes in aerosol sources in step with economic activity and emissions controls, most notably in East Asia and North America, give a longer timescale

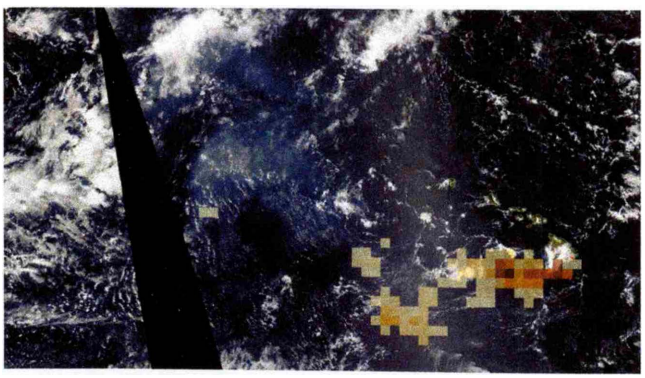

Figure 2.6 MODIS Aqua imagery of the 2008 eruption of Kīlauea, Hawaii. MODIS thermal anomalies are shown in red (impossible to see by eye in monochrome version). The OMI boundary layer SO_2 retrieval is overlaid in orange (large gray pixels in monochrome version).

during which the effects of aerosol and meteorological variability can be more cleanly separated (Bennartz, 2007; McCoy et al., 2018). Some examples of emissions controls that have had changes in cloud microphysics associated with them include the implementation in the United States of the 2009 Clean Air Interstate Rule and 2010 Acid Rain Program. In the People's Republic of China, similar controls include the twelfth 5-year Plan and preparations for the 2009 Beijing Olympic Games (McCoy et al., 2018). However, the slower nature of these changes introduces the confounding factors of internal variability and climate change (Manaster et al., 2017; Norris et al., 2016; Zelinka et al., 2020). The cycle of aerosol emissions between weekdays and weekends has also been suggested as a path toward assigning causality in ACI (Quaas et al., 2009). More generally, the contrast between polluted and pristine regions (Hamilton et al., 2014) may be considered to aggregate anthropogenic activity into a single opportunistic experiment (Koren et al., 2014; McCoy, McCoy, et al., 2020).

2.6.5. Ensemble Approaches to Uncertainty Quantification and Reduction in GCMs

General circulation models (GCMs) must represent ACIs to model Earth's climate and are also frequently used to study ACIs on large scales. Uncertainties in GCMs are associated with their initial conditions and internal variability, their "structural" representation of, or omission of, key processes, and their uncertain input datasets and parameters. The uncertainty associated with a subset of the uncertain input parameters, the "parametric uncertainty," can be quantified using perturbed parameter ensembles. In this approach, a large number of simulations are run with parameters varied, or inputs scaled, over plausible uncertainty ranges determined by the modeling team or other experts.

Some GCM ensembles aimed at ACI studies use designs where one parameter (or set of parameters) is varied at a time, and the effect of that parameter is determined directly (e.g., Lohmann & Ferrachat, 2010; Liu et al., 2018). Others vary many parameters at once and infer the importance of each parameter from subsequent analysis. This procedure allows interactions between parameters to be studied. It is feasible to vary around 50 parameters in today's GCMs in this way if around 200 GCM simulations of a year are integrated. To formally quantify the parametric uncertainty, tools such as Gaussian process emulation (see section 2.6.1) are then used to interpolate over the 50-dimensional parameter space and the range of model output variables such as radiative forcing in the emulated simulations is a measure of the parametric uncertainty in that output variable. Such techniques have been applied to understand parametric uncertainty in several climate models (e.g., Sexton et al., 2012; Qian et al., 2018). Focusing on ACIs, radiative forcing from the Twomey effect in a chemical transport model was calculated by Carslaw et al. (2013) and similar techniques were applied to a GCM ensemble described by Yoshioka et al. (2019) with a wider range of possible aerosol indirect forcing mechanisms by Regayre et al. (2018). These authors found that parametric uncertainty in the aerosol forcing is dominated by uncertainties in aerosol emissions and in the parameterization of clouds and their radiative effects. Studies of ACIs in a convective cloud model by Johnson et al. (2015) highlighted the high sensitivity of a convective cloud to aerosol concentrations and to the representation of cloud microphysics.

More recent work is focused on using observations to constrain the parameter space by eliminating implausible model variants, and thereby reducing uncertainty in the model output radiative forcing estimate (Johnson et al., 2020; Regayre et al., 2019; Watson-Parris et al., 2020). At the time of writing in 2021, these authors were able to reduce the uncertainty in their (ERF_{aci}) estimate by only 7%, though the direct aerosol effective radiative forcing uncertainty was reduced by 33%. Reducing the uncertainty is intrinsically difficult because not all parameters can be easily constrained and because each value of radiative forcing in the plausible range can be achieved with many different combinations of inputs, that is, a situation of *equifinality* (Lee et al., 2016). However, there is scope to reduce the uncertainty further by refining the statistical techniques and by using a more diverse set of complementary observations.

2.6.6. Regime Classification

The multiscaled nature of ACI means that patterns of space and time covariability cannot be restricted to a single length scale. One example is the structure of open and closed cellular convection in clouds (Fig. 2.7). This bi-stable morphology resembles Bernard-Rayleigh convection and occurs across the globe, but was not described until the first images of clouds from space revealed their structure (Agee, 1984). It is hypothesized that suppression of precipitation by aerosols may inhibit the transition from closed to open cells (Rosenfeld et al., 2006). This has been examined in satellite (Christensen et al., 2020; Goren & Rosenfeld, 2012, 2015) and aircraft (Abel et al., 2020) observations and in high-resolution simulations (Grosvenor et al., 2017; Possner et al., 2018). While structures such as open and closed cells present a simulation challenge at all but the highest resolutions (Kazil et al., 2011), machine learning presents an objective pathway toward classifying these convective regimes (Muhlbauer et al., 2014; McCoy, Wood, et al. 2017;

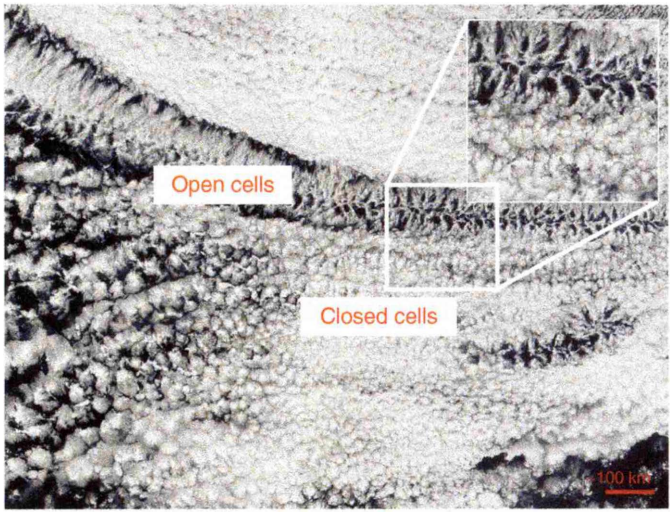

Figure 2.7 MODIS Terra imagery of open and closed cellular convection over the Pacific, 1 February 2016.

Wood & Hartmann, 2006). Recent analysis based on training a convolutional neural network provides a global examination of the properties of pockets of open cells, although it assigns a relatively slight radiative impact to closing all such pockets in the present-day (Watson-Parris et al., 2021).

Similar regime classification techniques exist for larger atmospheric structures, such as midlatitude cyclones. Approaches exist to identify cyclones and fronts (Field & Wood, 2007; Graf et al., 2017; Naud et al., 2010). Once the cyclones are isolated, the covariability of aerosol and clouds within them can be examined (Grandey, Stier, & Wagner, 2013; Grandey, Stier, Grainger, et al., 2013; Naud et al., 2017). Regime classification in large datasets of systems where variability in meteorological state and precipitation is substantial provides an opportunity to understand the causal linkages in the aerosol-cloud-precipitation system (McCoy et al., 2018). More complex regime classification techniques that characterize more of the frontal structure (Spensberger & Sprenger, 2018) are likely to yield additional insight into ACI occurring in this regime.

More broadly, k-means clustering offers a regime classification approach that can be applied to both observations and models with minimal assumptions (Williams & Webb, 2009). Application of this technique by Gryspeerdt and Stier (2012) demonstrated that the observationally inferred strength of ACIs (the sensitivity of N_d to aerosol optical depth, AOD) is greatest in the stratiform cloud regime, and this sensitivity was much more difficult to detect in cirrus and deep convective clouds. Further machine learning approaches to understanding clouds and climate are discussed in Chapter 16: Machine Learning for Clouds and Climate.

2.7. AEROSOL EFFECTS ON ICE AND MIXED-PHASE CLOUDS

Our discussion so far has focused on warm clouds; introducing the ice phase and generalizing to other cloud types lead to much additional complexity and associated uncertainty. Because warm clouds are shallow and their longwave emission temperatures are comparable to that of the surface, longwave radiative effects can usually be neglected in equation (2.12). For cirrus (Ci), in contrast, the longwave effect even dominates the shortwave effect (L'Ecuyer et al., 2019). To quantify aerosol effects on cold clouds, it is therefore necessary to extend equation (2.18) such that it accounts for perturbations to concentrations of ice nucleating particles (INP), the number of ice crystals N_i and ice water path. To date, a comprehensive quantification of the effects of aerosols on the radiative effects of cold clouds is missing, with available estimates largely limited to global modeling studies (Gettelman et al., 2012; Gryspeerdt et al., 2020; Heyn et al., 2017; Jensen & Toon, 1992; Lohmann et al., 2008; Penner et al., 2009). We therefore restrict our discussion to a qualitative overview of aerosol effects on cold clouds, as summarized in Table 2.1, but see also Chapter 4: Ice Particle Properties and Cirrus Emissivity. We do not discuss the details of the ice nucleation process or the role of INP chemical composition in it, and instead refer the reader to recent dedicated reviews by Murray et al. (2012) or Kanji et al. (2017).

We distinguish the formation of in situ cirrus from that of liquid-origin, or anvil cirrus. In situ Ci can form either *homogeneously*, that is, through homogeneous freezing of solution droplets, or *heterogeneously*, that is through deposition freezing onto the surfaces of INP. Both mechanisms for Ci formation can coexist and cloud response depends on their relative importance (e.g., Barahona et al., 2010; Gettelman et al., 2012; Zhu & Penner, 2020). Aerosol effects on Ci are strongest if the aerosol perturbation leads to a significant shift from homogeneous to heterogeneous ice nucleation because this means replacing the freezing of many solution droplets by ice nucleation on much fewer INP. The result is the formation of drastically fewer, but much larger ice crystals (Kärcher & Lohmann, 2003). The effect is enhanced by faster cloud dissipation through faster sedimentation of the larger crystals. A deliberate shift of homogeneous Ci formation to heterogeneous formation and faster sedimentation by seeding Ci with efficient INP has been discussed as a possible form of solar radiation management (Gasparini & Lohmann, 2016; Lohmann & Gasparini, 2017; Mitchell & Finnegan, 2009; Penner et al., 2015; Storelvmo et al., 2014). A third pathway of Ci formation is through the homogeneous freezing of liquid water droplets (in contrast to the solution

Table 2.1 Cloud response to aerosol perturbations by cloud and aerosol type. Cloud response is separated into the initial albedo response and adjustments. Processes targeted by suggestions for solar radiation management are highlighted by bold font, processes targeted by weather modification attempts in italics. Note that INP are considered non-soluble. See main text for details.

Cloud type	Aerosol type	Initial albedo response	Adjustments
Warm	CCN	**Higher albedo**	Entrainment-evaporation enhancement, **rain suppression/increased lifetime**
Homogeneous Ci	CCN	Slightly increased albedo	
Homogeneous Ci	INP	Lower albedo	**Faster sedimentation/reduced lifetime**
Heterogeneous Ci	INP	Slightly increased albedo	
Anvil Ci	CCN	Higher albedo	Slower sedimentation/increased lifetime
Mixed phase	INP	Glaciation/reduced albedo	*Faster precipitation formation/reduced lifetime/reduced orographic spill-over*
Mixed phase	CCN	Higher albedo	Evaporation/WBF enhancement, riming suppression
Deep convective	INP	Glaciation/reduced albedo due to glaciation	*Hail suppression*
Deep convective	CCN	Higher albedo	Decreased supersaturation/updraft invigoration, domain-wide adaptation of convective activity

droplets discussed earlier) in the anvil regions of deep convective clouds, which occurs at temperatures <−38°C. The number of cloud droplets available for homogeneous freezing depends on the number of CCN such that more but smaller droplets lead to more but smaller crystals (analogous to the Twomey effect) and anvils that persist longer due to reduced sedimentation velocities (Fan et al., 2013; Gryspeerdt, Mülmenstädt, et al., 2018; Morrison & Grabowski, 2011; Wang et al., 2020; Zhao et al., 2019). Increasing INP concentrations in a cloud that already freezes heterogeneously can also increase ice crystal number concentration (Zhou & Penner, 2014). Likewise, increasing the abundance of CCN/solution droplets in a homogeneous Ci may increase ice crystal number concentration (Gettelman et al., 2012; Gryspeerdt, Mülmenstädt, et al., 2018; Kärcher & Lohmann, 2003). Overall, however, the coupling of solution droplets and INP to Ci crystal number is much weaker in comparison to meteorological controls like updraft and temperature than for CCN and cloud droplet number (Gryspeerdt, Mülmenstädt, et al., 2018; Kärcher & Lohmann, 2002, 2003).

Ice crystals in mixed-phase clouds result from the freezing of cloud droplets that contain INP. For such crystals, the Wegener-Bergeron-Findeisen (WBF) (Bergeron, 1935; Findeisen, 1938; Storelvmo & Tan, 2015; Wegener, 1911) process leads to rapid growth of ice crystals at the expense of cloud water, that is, *glaciation* of the cloud. This means that ice crystal size is not controlled by the number of INP. The most important effect of perturbations to the INP concentration is therefore perturbations to the glaciation state, rather than changes in ice crystal size.

Glaciation frequently results in the formation of precipitation. *Glaciogenic cloud seeding*, that is, the deliberate introduction of efficient INP, usually silver iodide (Langmuir, 1950; Vonnegut, 1958), has thus been attempted as a means to shift orographic precipitation pattern from the leeward to the windward side of mountain ridges. While a chain of cloud processes observed during the SNOWIE field campaign (Tessendorf et al., 2019) has been documented (French et al., 2018), a statistically significant documentation of the efficiency of glaciogenic seeding remains challenging (Flossmann et al., 2019). Glaciogenic cloud seeding is also attempted to inhibit hail formation by favoring the ice-pathway of precipitation, that is, ice-ice collection and rimed snow, over the mixed-phase pathway leading to hail. A comprehensive series of experiments in Switzerland concluded the absence of a statistically significant effect of a randomized seeding strategy on hail kinetic energy (Federer et al., 1986), while a more recent study reports a significant effect for a moderately increased sample size and considering variability in seeding strength rather than randomized seeding (Dessens et al., 2006).

Pathways in mixed-phase precipitation formation can also be perturbed by an increase in CCN. Smaller cloud droplets reduce the efficiency of riming but increase evaporation, which in turn enhances the efficiency of the WBF process. Both sensitivities are notably weaker than that of autoconversion to droplet size (Glassmeier &

Lohmann, 2016). This is only one example of a tendency of adjustments in mixed-phase clouds to compensate each other, in line with the notion of clouds as *buffered* systems (Stevens & Feingold, 2009). Furthermore, the total amount of precipitation is subject to external constraints, which enforce a re-distribution of precipitation formation pathways in response to aerosol, rather than an overall change. For the example of stratiform orographic precipitation, such a constraint arises from the total condensation allowed for by orographic lifting (Glassmeier & Lohmann, 2018).

The effect of additional CCN on deep convective clouds has led to much debate. Considering individual updrafts, Rosenfeld et al. (2008) suggested an "ice-phase" pathway where smaller droplets would be more prone to cross the freezing level, which would result in convective invigoration through additional latent heat of freezing, and also precipitation formation and sedimentation. A recent theoretical study by Igel and van den Heever (2021) emphasizes the point made by Rosenfeld et al. (2008) and Grabowski and Morrison (2020) that the latent heat of freezing is approximately balanced, but slightly exceeded, by the energy needed to loft the condensate, so invigoration can actually only occur when the sedimentation of precipitation reduces the weight of the air parcel, making it more buoyant. Igel and van den Heever (2021) and Grabowski and Morrison (2016, 2020) agree that as a result the overall invigoration effect is often very weak.

Perhaps more effective is the "liquid-phase" pathway for convective invigoration described by Fan et al. (2007), Koren et al. (2014), Grabowski and Morrison (2016) and Fan et al. (2018). In this case, a convective invigoration is the result of additional latent heat of condensation due to a reduced in-cloud supersaturation under high-aerosol conditions. The invigoration, which is manifested in increased updraft speeds, can result in the "secondary" activation of aerosols well above the cloud base in comparison to unperturbed clouds. These aerosols were either too small to activate at cloud base or were entrained into the cloud from its edges. As these aerosols act to reduce the supersaturation, they may also feed back to affect the altitude at which the latent heat is released. However, isolating these complex effects of aerosols on deep convective clouds in observations is challenging, perhaps even impossible (Fan et al., 2018; Grabowski, 2018; Miltenberger et al., 2018).

When considering the embedding of convection in its environment beyond invigoration effects on individual cloud parcels (Morrison & Grabowski, 2013), the "embedding pathway" suggests that invigoration effects are likely restricted to localized areas rather than spread over entire regions (Abbott & Cronin, 2021; Morrison & Grabowski, 2013). Increased aerosol loading is also observed to lead to more, rather than stronger, convection (Abbott & Cronin, 2021; Blossey et al., 2018; Grabowski & Morrison, 2020). Grabowski and Morrison (2020) have associated this with mesoscale circulations, which they also suggest as a likely explanation for lightning enhancements in shipping lanes (Thornton et al., 2017). In a recent study, Abbott and Cronin (2021) moreover describe a "humidity-entrainment" mechanism for invigoration, which attributes invigoration to increased humidity caused by aerosol-enhanced detrainment and evaporation. As well as questioning the relevance of original "ice-phase" pathway for individual updrafts (Grabowski & Morrison, 2020), recent research has also suggested that invigoration effects are likely restricted to small areas rather than spread over entire regions (Abbott & Cronin, 2021).

2.8. SEMI-DIRECT EFFECTS

Semi-direct effects of aerosols on clouds were first so described by Hansen et al. (1997) and are associated with the effect of absorbing aerosols on local temperatures. The magnitude of the effects can be very large (tens of Wm^{-2}) locally, but both regional and global effects are poorly understood. The lack of understanding stems from two key sources: first, the effects depend strongly on the location of aerosols relative to clouds (Johnson et al., 2004), and second, calculation of semi-direct radiative effects requires an atmospheric model, and the simulated effects depend both on (frequently large) model biases in cloud cover and optical thickness and on internal variability.

Just a cloud droplet number concentrations are critical to understanding indirect effects, heating rates in the vicinity of clouds are critical to understanding semi-direct effects. Instantaneous heating rates generally range from 0.1 to 3 $Kday^{-1}$ (Gordon et al., 2018; Johnson, 2005; Panicker et al., 2014), which of course decrease substantially when annual or monthly means are considered (Allen et al., 2019). Local temperature changes resulting from the heating rates can reach up to a few Kelvin.

The effect of absorbing aerosols on cloud cover can be either positive or negative. Absorbing aerosols inside clouds can lead to clouds evaporating, while absorbing aerosols above temperature inversions can strengthen the temperature inversion by heating the air. This second effect can lead to additional cloud cover as the entrainment of dry air from above the boundary layer into clouds is reduced if the inversion is stronger (Gordon et al., 2018; Johnson et al., 2004; Koch & Del Genio, 2010). However, for above-cloud aerosols to have a strong effect, the aerosol layer must be very close to the cloud layer (Herbert et al., 2020). On the other hand, absorbing

aerosols below clouds can also enhance convection and therefore cloud cover in some cloud regimes (Feingold et al., 2005; McFarquhar & Wang, 2006).

Semi-direct effects are likely important in cloudy regions where concentrations of absorbing aerosols, mainly black carbon but also dust, are high. Regional studies have focused on three key areas, among others. In the Amazon rainforest, fires are frequent in the dry season, and different modeling studies find semi-direct effects of different signs (Archer-Nicholls et al., 2016; Feingold et al., 2005; Koren et al., 2004; Liu et al., 2020), and magnitudes of order 5 Wm^{-2} when averaged over a day or a few days. In the southeast Atlantic stratocumulus deck, which is in the outflow of the world's largest source of biomass burning aerosol in southern Africa, semi-direct effects could exceed 10 Wm^{-2} locally, but the sign is again uncertain (Gordon et al., 2018· Lu et al., 2018; Mallet et al., 2019; Yamaguchi et al., 2015). Similarly, large effects may prevail in very polluted and cloudy areas of South and East Asia (Menon et al., 2002) or nearby oceans (Ackerman, Toon, Stevens, et al., 2000). However, the semi-direct effects vary between and even within models, depending, for example, on whether convection is parameterized or explicit (Archer-Nicholls et al., 2016). The constraint that overlying aerosols must be close to cloud layers to exert negative semi-direct effects places challenging requirements on both models and observing instruments such as CALIOP, which are prone to errors of a few hundred meters in precisely locating the height of aer sol layers (Das et al., 2020; Rajapakshe et al., 2017; Shinozuka et al., 2020).

Global modeling studies are similarly diverse in their prediction of semi-direct effects, which is not surprising given that they often cannot even agree on direct effects of absorbing aerosol (Bond et al., 2013; Stier et al., 2013). Global modeling studies have frequently investigated semi-direct effects in the context of aerosol effects on atmospheric dynamics (Mahajan et al., 2012); in this context, they are a subset of "rapid adjustments." Recent Precipitation Driver and Response Model Intercomparison Project (PDRMIP) simulations with CMIP5 models found negative semi-direct effects of black carbon largely cancel positive direct effects (Stjern et al., 2017). However, one noteworthy study (Allen et al., 2019) attempts to reduce model biases via observational constraints and finds semi-direct effects are globally positive, in contrast to the CMIP5 models. These global model intercomparisons also highlight the importance of semi-direct effects on high clouds in climate models, which may be a promising avenue for future work with more detailed models. More generally, the lack of consensus even on how semi-direct effects influence low clouds invites additional modeling and observational studies at a range of scales.

2.9. FIELD EXPERIMENTS

For decades, field campaigns have been conducted to better understand ACIs. Usually, these involve either aircraft or surface measurements or both, although tethered or untethered balloons, drones or airships are also promising as the slower pace permits more detailed sampling of individual clouds. The scale and scope of ACI-focused field campaigns has steadily increased since early observations of CCN by Woodcock (01 Oct. 1953) and others, who collected the aerosols on glass slides mounted on their aircraft, or sometimes stretched spider's webs (Twomey, 1954). Here, we discuss only a selection of the most recent field campaigns dedicated to ACIs for which major scientific outcomes are known, with apologies for the inevitable omissions.

The important role of CCN in determining the properties of low clouds at low latitude was investigated in campaigns in the southeast Atlantic between 2016 and 2018 (Zuidema et al., 2016). In the ORACLES (Redemann et al., 2021), CLARIFY (Haywood et al., 2021), LASIC (Zuidema et al., 2018), and AEROCLO-sa (Formenti et al., 2019) campaigns, the effect of smoke plumes from Africa on the important stratocumulus·to-cumulus transition in the region is potentially critical to their radiative effects (Yamaguchi et al., 2015; Zhou et al. 2017). A highlight of these campaigns for ACIs was the demonstration that entrainment of free tropospheric air masses into the boundary layer can be suppressed by pockets of open cells (Abel et al., 2020).

Low-level clouds at low latitudes have also been targeted by the EUREC^{4}A, and ATOMIC campaigns in the Barbados trade cumulus region (Bony et al., 2017; Stevens et al., 2021) were more focused on clouds than aerosols, but their extremely large-scale (four aircraft, four research vessels, two unmanned aerial vehicles [UAVs], and a surface station) and broad-scope meant ACIs were also investigated. We anticipate insights into the role of Saharan dust in suppressing precipitation in trade cumulus clouds (Stevens et al., 2021).

At the crossover point from low-latitudes to midlatitudes, the ACE-ENA campaign from the Azores in 2017 and 2018 (Zheng et al., 2021) studied both marine stratocumulus and clouds associated with extra-tropical cyclones. The current ACTIVATE campaign is also likely to yield new insights into low-level clouds, also in the North Atlantic, but further north and west in a similar region to that sampled by the NAAMES campaign (Behrenfeld et al., 2019). Concurrently, a series of field experiments (CAPRICORN, SOCRATES, MARCUS, and MICRE) probed low clouds in the Southern Ocean (McFarquhar et al., 2020). So far, a common theme of all of these campaigns has been how clouds can create favorable environments for the formation of new aerosol

particles (McCoy et al., 2021; Sanchez et al., 2018; Zheng et al., 2021), which may subsequently grow to act as CCN. The proposed mechanism in the subtropics (at the Azores) involves new particle formation in clean regions of the upper boundary layer, while in the Southern Ocean and north-western North Atlantic it appears to happen at higher altitude, facilitated by upward transport of precursors, perhaps in midlatitude cyclones.

The Southern Ocean campaigns also made extensive measurements of INP concentrations and found them to be much lower than observed earlier by Bigg (1973). INP concentrations are hypothesized to be an important contributor to climate model biases in the region (Murray et al., 2021; Vergara-Temprado et al., 2018). The deficiency of supercooled liquid in the Southern Ocean is now addressed in the latest climate model simulations informed by these field campaigns (Gettelman et al., 2020). Likewise in the northern latitudes, ongoing analysis of the MOSAIC campaign data from the RV Polarstern, which drifted in Arctic ice over the 2019–2020 winter season, is likely to yield additional insights into the role of ACIs in the rapidly changing Arctic climate.

Deep clouds and their interactions with aerosols have also been studied extensively recently, though aircrafts do not usually sample convective cores so in situ measurements are more limited. The synergistic Go-Amazon and ACRIDICON-CHUVA campaigns in the Amazon elucidated the aerosol-cloud life cycle in the Amazon rainforest (Andreae et al., 2018; Wang & Zhang, 2016). As in the more recent ATom campaigns (Williamson et al., 2019), intense new particle formation in the upper troposphere was observed and hypothesized to supply CCN to boundary-layer clouds. The significance of upper-tropospheric aerosol production processes for clouds was appreciated earlier by Clarke et al. (1998) and others but it can now be studied in unprecedented detail, and is one aim of the CAFÉ-Brazil mission of 2022. Complementary measurements of ACIs in deep clouds have been collected more recently by the CAMP^{2}EX mission in fall 2019, which has studied cloud effects on aerosol in air masses near the Maritime Continent (Hilario et al., 2021). Early data suggest wet scavenging is a dominant process shaping aerosol size distributions in the free troposphere.

Aircraft measurements yielding detailed in situ information are complemented by short- and long-term remote sensing from the surface as well as from space (section 2.10). Sometimes, clouds can be sampled directly in this way: in fog, detailed in situ measurements can be obtained at the surface over long periods directly. Two recent notable field campaigns on aerosol-fog interactions are C-FOG in eastern Canada (Fernando et al., 2021) focused on coastal fog and WIFEX in the Indo-Gangetic Plain between 2015 and 2019 (Ghude et al., 2017). While a critical research question in all fog studies concerns the activation of aerosol at low supersaturation (e.g., Mazoyer et al., 2019), this is complicated in the severely polluted environment of the Indo-Gangetic Plain by high concentrations of absorbing aerosol (Safai et al., 2019) which could potentially lead to changes in supersaturation due to heating effects.

When clouds are higher, surface remote sensing measurements using radar, lidar, and microwave techniques are key to long-term studies of ACIs. The most prominent surface remote sensing measurements are those of the US Department of Energy's ARM program, now in its 28th year of operations (Mather & Voyles, 2013), which now has three permanent stations at the Southern Great Plains, North Slope of Alaska, and Graciosa Island sites as well as several mobile facilities which participated in, or were the focus of, some of the campaigns listed above, namely, LASIC, MOSAIC, and MARCUS. The increased precision and sophistication of cloud radars (Kollias et al., 2020), improved calculations of cloud microphysical properties from surface retrievals (e.g., Wu et al., 2020; Yang et al., 2019), and the introduction of tethered balloon measurements (Dexheimer et al., 2019) are likely the most exciting recent innovations for studies of ACIs.

2.10. NEW SATELLITE PRODUCTS

Many of the techniques for constraining ACI we describe in earlier sections rely on satellite retrievals. Satellite observations are attractive for several reasons: they can provide observations of remote, pristine regions that are critical in setting forcing from ACI (Carslaw et al., 2013; Hamilton et al., 2014; McCoy, McCoy et al., 2020), their large data volume allows detection of relatively small amounts of ACI-induced variability relative to meteorologically-induced variability (Bender et al., 2019); and they can allow long-term observations of regions that reveal trends and responses to transient events (Bennartz et al., 2011; Li et al., 2018; McCoy et al., 2018; Malavelle et al., 2019). We will briefly survey common satellite observations used in evaluating ACI.

Constraint of the first indirect effect in liquid clouds by satellite requires knowledge of aerosol that is relevant to CCN and the cloud microphysical state (Nakajima et al., 2001; Quaas et al., 2020). While passive near-IR and visible retrievals by satellites are sensitive to cloud droplet radius(r_e), the more physically informative variable describing ACI in warm clouds is N_d (Wood, 2012) (see section 2.4). This quantity can be calculated with some assumptions using retrievals of τ and r_e (Bennartz & Rausch, 2017; Grosvenor et al., 2018; Grosvenor & Wood, 2014; Nakajima et al., 2001) (section 2.4). However, these calculations require that clouds be plane-parallel, which

may potentially lead to substantial regional and seasonal biases (Grosvenor & Wood, 2014; Zhang et al., 2016, 2019). Similar retrievals are possible utilizing microwave LWP (Bennartz, 2007), polarimeter droplet radius (Alexandrov et al., 2012; Hasekamp et al., 2019), and lidar ob ervations of optical depth (Hu et al., 2007; Li et al., 2018). Each of these retrievals has assumptions that are made in the retrieval process and thus strengths and weaknesses relative to other retrievals (Grosvenor et al., 2018). Observations of aerosol properties from space are possible and may be coupled with observations of N_d to yield an estimate of the first indirect effect (Gryspeerdt et al., 2017· Nakajima et al., 2001· Quaas et al., 2020). However, the use of vertically integrated aerosol can be problematic when aerosol and clouds are not vertically collocated. Furthermore, when aerosol and cloud are vertically collocated, aerosol swelling by cloud substantially complicates the relationship of AOD to aerosol number concentration (Christensen et al., 2017; Twohy et al., 2009), and this and other sources of bias tend to be most important in clean regimes where clouds are most sensitive to aerosols (Ma et al., 2018). As an alternative, studies have utilized aerosol reanalysis that attempt to account for near-cloud aerosol swelling (Bellouin et al., 2013; McCoy, Bender, et al., 2017) or have screened aerosol retrievals for nearby cloud (Christensen et al., 2017).

Constraints on aerosol-cloud adjustments in liquid clouds require knowledge of cloud macrophysical state and microphysical state (Albrecht, 1989; Gryspeerdt, Goren, et al., 2019). As discussed above, N_d is the most relevant variable relating to microphysical state. However, inference of the sensitivity of cloud macrophysical state to N_d is complicated due to non-distinct causality (see sections 2.6.3 and 2.6.4). The most common satellite observations of warm cloud properties considered are in-cloud LWP (Malavelle et al., 2019; Gryspeerdt, Goren, et al., 2019), cloud areal extent (Albrecht, 1989; Gryspeerdt et al., 2016), and area-mean LWP (McCoy et al., 2018; McCoy, Field, 2020). This list is by no means conclusive and other quantities less directly related to shortwave radiative forcing have been examined, such as cloud top height (Mace & Abernathy, 2016). These properties may be derived from a multitude of different satellite instruments, although they are most commonly examined in the context of passive spectroradiometers such as the MODIS (Platnick et al., 2003). However, it has been argued that passive microwave observations of liquid water path (Elsaesser et al., 2017) share less information with N_d calculated from τ and r_e, are more directly comparable to GCMs, and are less sensitive to cloud heterogeneity (McCoy, Field, et al., 2020). On the other hand, the fact that microwave liquid water path observations do not share shortwave scattering information with the calculation of N_d also means that they are less directly related to the shortwave radiative properties, such as cloud fraction and τ, which are primarily derived from visible wavelength light.

Satellite-based inferences of the aerosol effect on cold clouds are much more difficult to make than inferences of effects on warm clouds, and the effect of ice-phase microphysics on ERF_{aci} is thought to be small relative to liquid (Bellouin et al., 2020). However, lidar (e.g., CALIOP) and combined lidar and radar (e.g., Cloudsat) observations of cloud phase and ice crystal number concentration show covariation with dust, indicative of glaciation, as well as potential signatures of INP (Gryspeerdt, Sourdeval, et al. 2018; Sourdeval et al., 2015, 2016 2018; Hu et al., 2010; Tan et al., 2014). Observations of ice water content and path are still highly uncertain, but can be made using both passive and active observations (Jiang et al., 2012).

2.11. OUTLOOKS

Radiative forcing by ACIs has been considered quantitatively by Wigley (1989) and then by the Second IPCC Assessment Report, where it was assessed to be between -1.5 and $0\,Wm^{-2}$. Top-down constraints such as the temperature differences between hemispheres, the observed temperature record, as well as sulfur flux estimates (Schwartz, 1988) were all employed. The radiative forcing due to the first indirect effect is referred to as RF_{aci} and the forcing including "rapid adjustments," which include cloud adjustments to aerosols or "second indirect effects" is referred to as effective radiative forcing or ERF_{aci} (Boucher et al., 2014). In 2020, the ERF_{aci} from 1850 to the present-day was estimated by Bellouin et al. (2020) as between -1.73 and $-0.27\,Wm^{-2}$ (16–84% range), based mainly on global modeling and satellite-derived estimates. When top-down considerations are included, the overall aerosol forcing range becomes -2.0 to $-0.35\,Wm^{-2}$, this time a 5–95% confidence interval including aerosol-radiation interactions. A subset of CMIP6 models yield a similar estimate of -1.41 to $-0.21Wm^{-2}$ (Smith et al., 2020). To obtain the uncertainty range quoted here, we have simply doubled the standard deviation of the different models calculated by Smith et al. (2020) to approximate the 5–95% confidence interval. This uncertainty from the multi-model intercomparison is slightly smaller than the Bellouin et al. (2020) estimate, but may grow as more models participate. It also does not account for the large uncertainties in emissions inventories, which are prescribed for the intercomparison and are therefore identical between models, nor does it account for correlation between models (Knutti et al., 2010). Some approaches yield much the same results but some do not. For example, McCoy, McCoy, et al. (2020) obtain

an estimate for the RF_{aci} of -1.6 to $-0.6\,Wm^{-2}$ by contrasting the Northern and Southern Hemispheres, but the estimate obtained by Johnson et al. (2020) from an uncertainty quantification exercise on a single GCM of -2.88 to $-1.28\,Wm^{-2}$ (5 – 95%) is rather larger and the central value is significantly more negative. The uncertainty thus remains high, but should decrease as anthropogenic emissions are reduced and the central value of the present-day forcing becomes less negative. As this central value decreases, global temperature rise will accelerate (Andreae et al., 2005), although perhaps not substantially (Shindell & Smith, 2019). Either way, the feasibility of a controlled utilization of ACIs in geoengineering approaches to temporarily moderate temperature rise may need to be explored (National Academies of Sciences & Medicine, 2021). Here, "feasibility" has to be understood in the broadest sense, ranging from the level of cloud physics via our modeling capabilities of unintended side effects to the level of governance and ethics.

Solar radiation management by stratospheric aerosol injection is associated with risks to the ozone layer or to long-term biogeochemical cycles. Marine cloud brightening (Latham, 2002; Latham et al., 2012), in contrast, is based on an easily reversible intervention, whose exploration has, moreover, large overlap with improving our fundamental understanding of ACI in stratocumulus. While small-scale marine cloud brightening experiments would offer a laboratory for ACI studies (Wood & Ackerman, 2013; Wood et al., 2017), an improved understanding of ACI directly informs the feasibility and limitations of marine cloud brightening strategies (Glassmeier et al., 2021). The main problems associated with marine cloud brightening from a geoengineering perspective are that it is not clear whether the technique would be sufficiently effective in enhancing cloud albedo, and it might, at least temporarily, disturb tropospheric circulation. However, we expect to see significant new work in the coming decade.

There are some other potential avenues for breaking the deadlock in ACI research to reduce the forcing uncertainty. New records of pre-industrial aerosols may come to light, for example, in ice cores (Carslaw et al., 2017) or less obvious sources such as historical artworks (Gryspeerdt, 2019; Zerefos et al., 2014). Global cloud resolving models (Stevens et al., 2019) are likely critical to understanding both forcing and feedbacks (Schneider et al., 2017; Terai et al., 2020). The incorporation of fully prognostic aerosols in such models is also under way either by testing aerosols and ACIs in various kinds of multiscale models (Gordon et al., 2020; Wang et al., 2011; Zhang et al., 2012), or by running global models with aerosols at progressively higher resolution. To our knowledge, the highest spatial grid resolution of a global model with prognostic aerosols is 3.5 km for a 2-week integration (Sato et al., 2016).

New machine learning approaches to better understand the proliferation of data that we already have are likely to play a major role in reducing forcing uncertainty, but require caution as results from machine learning algorithms are only as good as the data or models that are used to train and test them. For example, parametric uncertainty quantification says nothing about uncertainties or biases that cannot be easily parameterized, so can only ever predict part of the full uncertainty. Happily, it is a complementary part of the uncertainty to that previously explored by comparing different models. Machine learning can also be embedded in models directly to allow some processes to be treated more efficiently or with more complexity (e.g., Brenowitz & Bretherton, 2018; Krasnopolsky et al., 2005). While these approaches are challenging, due, for example, to the need to satisfy conservation laws and other basic requirements of physical models, constraints to overcome these problems are rapidly being developed (e.g., Beucler et al., 2021), paving the way toward more widespread adoption of promising machine learning algorithms.

As global temperatures climb, we foresee two further topics gaining new importance. The first is aerosol effects on cloud feedbacks. Gettelman et al. (2016) showed that different aerosol concentrations in the same model can lead to different cloud feedbacks as well as different radiative forcing and demonstrated the use of an "aerosol kernel," inspired by the radiative kernels of Soden et al. (2008), to disentangle forcing and feedbacks. Mathematically and conceptually, this kernel has some similarities to susceptibility. The second topic is the role of ACIs in weather forecasting and environmental engineering research. While both weather and climate modification techniques are rightly controversial, the interest in seeding of precipitation in clouds (French et al., 2018) is likely to grow as the planet warms and many formerly fertile areas are likely to become arid and barren. It may thus become crucial to revisit questions of the theoretical and practical feasibility of weather modification. Similarly, marine cloud brightening (Latham, 2002) may be seen as a potential way to leverage ACIs to influence regional climate. Semi-direct effects affect weather in heavily polluted regions (Ding et al., 2013; Gautam et al., 2007; Ma et al., 2020) and numerical weather prediction models are increasingly catching up with climate models in adopting more sophisticated aerosol schemes (Benedetti & Vitart, 2018). Widespread inclusion of ACIs in weather forecasting models is still on the horizon, but becomes more feasible every year.

Thus, despite the likelihood that global aerosol loadings decrease in the coming decades, ACIs will remain important. Continued efforts to understand them better

will likely be repaid many times over with substantially improved capabilities for environmental prediction at all spatial and temporal scales.

ACKNOWLEDGMENTS

We are grateful to Leighton Regayre for discussions. Hamish Gordon acknowledges the support of Carnegie Mellon University and the NASA Roses program under grant number 80NSSC19K0949. Daniel McCoy acknowledges the support of the University of Wyoming. Franziska Glassmeier acknowledges support from The Branco Weiss Fellowship Society in Science, administered by the ETH Zürich, and from a Veni grant of the Dutch Research Council (NWO).

REFERENCES

Abbott, T. H., & Cronin, T. W. (2021). Aerosol invigoration of atmospheric convection through increases in humidity. *Science*, *371*(6524), 83–85. doi: 10.1126/science.abc5181

Abdul-Razzak, H., & Ghan, S. J. (2000, Mar). A parameterization of aerosol activation: 2. Multiple aerosol types. *Journal of Geophysical Research: Atmospheres*, *105*(D5), 6837–6844. doi: 10.1029/1999JD901161

Abel, S. J., Barrett, P. A., Zuidema, P., Zhang, J., Christensen, M., Peers, F., et al. (2020). Open cells exhibit weaker entrainment of free-tropospheric biomass burning aerosol into the south-east Atlantic boundary layer. *Atmospheric Chemistry and Physics*, *20*(7), 4059–4084. doi: 10.5194/acp-20-4059-2020

Ackerman, A. S., Kirkpatrick, M. P., Stevens, D. E., & Toon, O. B. (2004, Dec). The impact of humidity above stratiform clouds on indirect aerosol climate forcing. *Nature*, *432*(7020), 1014–1017. doi: 10.1038/nature03174

Ackerman, A. S., Toon, O. B., Stevens, D. E., Heymsfield, A. J., Ramanathan, V., & Welton, E. J. (2000). Reduction of tropical cloudiness by soot. *Science*, *288*(5468), 1042–1047. doi: 10.1126/science.288.5468.1042

Ackerman, A. S., Toon, O. B., Taylor, J. P., Johnson, D. W., Hobbs, P. V., & Ferek, R. J. (2000, Aug). Effects of aerosols on cloud albedo: Evaluation of Twomey's parameterization of cloud susceptibility using measurements of ship tracks. *Journal of the Atmospheric Sciences*, *57*(16), 2684–2695. doi: 10.1175/1520-0469(2000)057⟨2684: EOAOCA⟩2.0.CO;2

Agee, E. M. (1984). Observations from space and thermal convection: An historical perspective. *Bulletin of the American Meteorological Society*, *65*(9), 938–949. doi: 10.1175/1520-0477(1984)065⟨0938:ofsatc⟩2.0.co;2

Aitken, J. (1881). *Dust, fogs, and clouds* (Vol. 23) (o. 591). Nature Publishing Group, 384–385. doi: 10.1038/023384a0

Albrecht, B. A. (1989, Sep). Aerosols, cloud microphysics, and fractional cloudiness. *Science*, *245*(4923), 1227–1230. doi: 10.1126/science.245.4923.1227

Alexandrov, M. D., Cairns, B., Emde, C., Ackerman, A. S., & van Dieden-hoven, B. (2012 Oct). Accuracy assessments of cloud droplet size retrievals from polarized reflectance measurements by the research scanning polarimeter. *Remote Sensing of Environment*, *125*, 92–111. doi: 10.1016/j.rse.2012.07.012

Allen, R. J., Amiri-Farahani, A., Lamarque, J.-F., Smith, C., Shindell, D., Hassan, T., & Chung, C. E. (2019). Observationally constrained aerosol–cloud semi-direct effects. *NPJ Climate and Atmospheric Science*, *2*(1). doi: 10.1038/s41612-019-0073-9

Andreae, M. O., Afchine, A., Albrecht, R. Holanda, B. A., Artaxo, P., Barbosa, H. M. J., et al. (2018, Jan). Aerosol characteristics and particle production in the upper troposphere over the Amazon Basin. *Atmospheric Chemistry and Physics*, *18*(2), 921–961. doi: 10.5194/acp-18-921-2018

Andreae, M. O., Jones, C. D., & Cox, P. M. (2005, June). Strong present-day aerosol cooling implies a hot future. *Nature*, *435*(7046), 1187–1190. doi: 10.1038/nature03671

Archer- icholls, S., Lowe, D., Schultz, D. M., & McFiggans, G. (2016). Aerosol– radiation-cloud interactions in a regional coupled model: The effects of convective parameterisation and resolution. *Atmospheric Chemistry and Physics*, *16*(9), 5573–5594. doi: 10.5194/acp-16-5573-2016

Axford, D. . (1968, Aug). On the accuracy of wind measurements using an inertial platform in an aircraft, and an example of a measurement of the vertical mesostructure of the atmosphere. *Journal of Applied Meteorology*, *7*(4), 645–666. doi: 10.1175/1520-0450(1968)007

Barahona, D., Rodriguez, J., & enes, A. (2010). Sensitivity of the global distribution of cirrus ice crystal concentration to heterogeneous freezing. *Journal of Geophysical Research: Atmospheres*, *115*(D23). doi: https://doi.org/10.1029/2010JD014273

Baumgardner, D. Jonsson, H. Dawson W., O'Connor, D., & Newton, R. (2001, Oct). The cloud, aerosol and precipitation spectrometer: A new instrument for cloud investigations. *Atmospheric Research*, *59–60*, 251–264. doi: 10.1016/S0169-8095(01)00119-3

Behrenfeld, M. J., Moore, R. H., Hostetler, C. A. Graff, J., Gaube, P., Russell, L. M., et al. (2019). The orth Atlantic Aerosol and Marine Ecosystem Study (AAMES): Science motive and mission overview. *Frontiers in Marine Science*, *6*, 122. doi: 10.3389/fmars.2019.00122

Bellouin, ., Mann, G. W., Woodhouse, M. T., Johnson, C., Carslaw, K. S., & Dalvi, M. (2013 Mar). Impact of the modal aerosol scheme GLOMAP-mode on aerosol forcing in the Hadley Centre Global Environmental Model. *Atmospheric Chemistry and Physics*, *13*(6), 3027–3044. doi: 10.5194/acp-13-3027-2013

Bellouin, ., Quaas, J., Gryspeerdt, E. Kinne, S., Stier, P., Watson-Parris, D., Stevens B. (2020, Mar). Bounding global aerosol radiative forcing of climate change. *Reviews of Geophysics*, *58*(1), e2019RG000660. doi: 10.1029/2019RG000660

Bender, F.-M., Frey, L., McCoy, D. T., Grosvenor, D. P., & Mohrmann, J. K. (2019). Assessment of aerosol-cloud–radiation correlations in satellite observations, climate models and reanalysis. *Climate Dynamics*, *52*(7–8), 4371–4392.

Benedetti, A. & Vitart, F. (2018, Oct). Can the direct effect of aerosols improve subseasonal predictability? *Monthly*

Weather Review, *146*(10), 3481–3498. doi: 10.1175/MWR-D-17-0282.1

Bennartz, R. (2007, Jan). Global assessment of marine boundary layer cloud droplet number concentration from satellite. *Journal of Geophysical Research*, *112*(D2), D02201. doi: 10.1029/2006JD007547

Bennartz, R., Fan, J., Rausch, J., Leung, L. R., & Heidinger, A. K. (2011). Pollution from China increases cloud droplet number, suppresses rain over the East China Sea. *Geophysical Research Letters*, *38*(9). doi: 10.1029/2011gl047235

Bennartz, R., & Rausch, J. (2017, Aug). Global and regional estimates of warm cloud droplet number concentration based on 13 years of AQUA-MODIS observations. *Atmospheric Chemistry and Physics*, *17*(16), 9815–9836. doi: 10.5194/acp-17-9815-2017

Bergeron, T. (1935). On the physics of cloud and precipitation. In *Procés-verbaux des séances de l'Association de Météorologie (Cinquiéme assemblée générale, Lisbonne)* (Vol. II: Mémoires, pp. 156–178). Imprimerie Paul Dupont.

Beucler T., Pritchard, M., Rasp, S., Ott, J., Baldi, P., & Gentine, P. (2021, Mar). Enforcing analytic constraints in neural networks emulating physical systems. *Physical Review Letters*, *126*, 098302. doi: 10.1103/PhysRevLett.126.098302

Bigg, E. K. (1973, Sept). Ice nucleus concentrations in remote areas. *Journal of Atmospheric Sciences 30*(6), 1153–1157. doi: 10.1175/ 1520-0469(1973)030⟨1153:INCIRA⟩2.0.CO;2

Blossey, P. ., Bretherton, C. S., Thornton, J. A., & Virts, K. S. (2018). Locally enhanced aerosols over a shipping lane produce convective invigoration but weak overall indirect effects in cloud-resolving simulations. *Geophysical Research Letters*, *45*(9305–9313).

Bond, T. C., Doherty, S. J., Fahey, D. W., Forster, P. M., Berntsen, T., Deangelo, B. J., et al. (2013, Jun). Bounding the role of black carbon in the climate system: A scientific assessment. *Journal of Geophysical Research Atmospheres*, *118*(11), 5380–5552. doi: 10.1002/jgrd.50171

Bony, S., Stevens, B., Ament, F., Bigorre, S., Chazette, P., Crewell, S., et al. (2017, Nov). EUREC^{4}A: A field campaign to elucidate the couplings between clouds, convection and circulation. *Surveys in Geophysics*, *38*(6), 1529–1568. doi: 10.1007/s10712-017-9428-0

Boucher, O., & Lohmann, U. (1995). The sulfate-CCN-cloud albedo effect. *Tellus B*, *47*(3), 281–300. doi: https://doi.org/10.1034/j.1600-0889.47.issue3.1.x

Boucher, O., Randall, D., Artaxo, P., Bretherton, C., Feingold, G., Forster, P., et al. (2014). Clouds and aerosols. In T. Stocker et al. (Eds.), *Climate Change 2013 – The Physical Science Basis: Working Group I Contribution to the Fifth Assessment Report of the Intergovernmental Panel on Climate Change* (p. 571–658). Cambridge University Press. doi: 10.1017/CBO9781107415324.016

Brenowitz, N. D., & Bretherton, C. S. (2018, Jun). Prognostic validation of a neural network unified physics parameterization. *Geophysical Research Letters*, *45*(12), 6289–6298. doi: 10.1029/2018GL078510

Bretherton, C. S., Blossey, P. N., & Uchida, J. (2007). Cloud droplet sedimentation, entrainment efficiency, and subtropical stratocumulus albedo. *Geophysical Research Letters*, *34*(3). doi: 10.1029/2006GL027648

Carn, S. A., Fioletov, V. E., McLinden, C. A., Li, C., & Krotkov, . A. (2017). A decade of global volcanic SO_2 emissions measured from space. *Scientific Reports*, *7*, 44095. doi: 10.1038/srep44095https://www.nature.com/articles/srep44095#supplementary-information

Carslaw, K. S., Boucher, O., Spracklen, D. V., Mann, G. W., Rae, J. G. L., Woodward, S., & Kulmala, M. (2010, Feb). A review of natural aerosol interactions and feedbacks within the Earth system. *Atmospheric Chemistry and Physics*, *10*(4), 1701–1737. doi: 10.5194/acp-10-1701-2010

Carslaw, K. S., Gordon, H., Hamilton, D. S., Johnson, J. S., Regayre, L. A., Yoshioka, M., & Pringle, K. J. (2017, Mar). Aerosols in the pre-industrial atmosphere. *Current Climate Change Reports*, *3*(1), 1–15. doi: 10.1007/ s40641-017-0061-2

Carslaw, K. S., Lee, L. A., Reddington, C. L., Mann, G. W., & Pringle, K. J. (2013, Dec). The magnitude and sources of uncertainty in global aerosol. *Faraday Discussions*, *165*, 495–512. doi: 10.1039/c3fd00043e

Charlson, R. J., Schwartz, S. E., Hales, J. M., Cess, R. D., Coakley, J. A., Hansen, J. E., & Hofmann, D. J. (1992, Jan). Climate forcing by anthropogenic aerosols. *Science*, *255*(5043), 423–430. doi: 10.1126/science.255.5043.423

Chen, Y.-C., Christensen, M. W., Stephens, G. L., & Seinfeld, J. H. (2014). Satellite-based estimate of global aerosol-cloud radiative forcing by marine warm clouds. *Nature Geoscience*, *7*, 643–646.

Christensen, M., Gettelman, A., Cermak, J., Dagan G., Diamond, M., Douglas, A., et al. (2021). Opportunistic experiments to constrain aerosol effective radiative forcing. *Atmospheric Chemistry and Physics, 2021*, 1–60. doi: 10.5194/acp-2021-559

Christensen M. W., Jones, W. K., & Stier, P. (2020, Jul). Aerosols enhance cloud lifetime and brightness along the stratus-to-cumulus transition. *Proceedings of the National Academy of Sciences*, *117*(30), 17591–17598.

Christensen, M. W., Neubauer, D., Poulsen, C. A., Thomas, G. E., McGarragh, G. R., Povey, A. C., et al. (2017). Unveiling aerosol–cloud interactions. Part 1: Cloud contamination in satellite products enhances the aerosol indirect forcing estimate. *Atmospheric Chemistry and Physics*, *17*(21), 13151–13164. doi: 10.5194/acp-17-13151-2017

Chuang, P. Y., Nenes, A., Smith, J. N., Flagan, R. C., & Seinfeld, J. H. (2000, Aug). Design of a CCN instrument for airborne measurement. *Journal of Atmospheric and Oceanic Technology*, *17*(8), 1005–1019. doi: 10.1175/1520-0426(2000)017⟨1005:DOACIF⟩2.0.CO;2

Clarke, A. D., Varner, J. L., Eisele, F., Mauldin, R. L., Tanner, D., & Litchy, M. (1998, Jul). Particle production in the remote marine atmosphere: Cloud outflow and subsidence during ACE 1. *Journal of Geophysical Research: Atmospheres*, *103*(D13), 16397–16409. doi: 10.1029/97JD02987

Conover, J. H. (1966, Nov). Anomalous cloud lines. *Journal of Atmospheric Sciences*, *23*(6), 778–785. doi: 10.1175/1520-0469(1966)023⟨0778:ACL⟩2.0.CO;2

Dagan, G., Koren, I., & Altaratz, O. (2015). Aerosol effects on the timing of warm rain processes. *Geophysical Research Letters*, *42*(11), 4590–4598. doi: https://doi.org/10.1002/2015GL063839

Das, S., Colarco, P. R., & Harshvardhan, H. (2020, Mar). The influence of elevated smoke layers on stratocumulus clouds over the SE Atlantic in the NASA Goddard Earth Observing System (GEOS) model. *Journal of Geophysical Research: Atmospheres*, *125*(6). doi: 10.1029/2019JD031209

Dessens, J., Berthet, C., & Sanchez, J. L. (2006). A sensitivity test for hail prevention assessment with hailpad measurements. *Journal Weather Modification*, *38*, 44–50.

Dexheimer, D., Airey, M., Roesler, E., Longbottom, C., Nicoll, K., Kneifel, S., et al. (2019). Evaluation of arm tethered-balloon system instrumentation for supercooled liquid water and distributed temperature sensing in mixed-phase arctic clouds. *Atmospheric Measurement Techniques*, *12*(12), 6845–6864. doi: 10.5194/amt-12-6845-2019

Diamond, M. S., Director, H. M., Eastman, R., Possner, A., & Wood, R. (2020). Substantial cloud brightening from shipping in subtropical low clouds. *AGU Advances*, *1*(1), e2019AV000111.

Ding, A. J., Fu, C. B., Yang, X. Q., Sun, J. ., Petäjä, T., Kerminen, V.-M., et al. (2013). Intense atmospheric pollution modifies weather: A case of mixed biomass burning with fossil fuel combustion pollution in eastern China. *Atmospheric Chemistry and Physics*, *13*(20), 10545–10554. doi: 10.5194/acp-13-10545-2013

Dusek, U., Frank, G. P., Hildebrandt, L., Curtius, J., Schneider, J., Walter, S., et al. (2006, Jun). Size matters more than chemistry for cloudnucleating ability of aerosol particles. *Science*, *312*(5778), 1375–1378. doi: 10.1126/science.1125261

Elsaesser, G. S., O'Dell, C. W., Lebsock, M. D., Bennartz, R., Greenwald, T. J., & Wentz, F. J. (2017). The Multi-Sensor Advanced Climatology of Liquid Water Path (MAC-LWP). *Journal of Climate*, *30*(24), 10193–10210. doi: 10.1175/jcli-d-16-0902.1

Engstrom, A., Bender, F. A. M., Charlson, R. J., & Wood, R. (2015). Geographically coherent patterns of albedo enhancement and suppression associated with aerosol sources and sinks. *Tellus B: Chemical and Physical Meteorology*, *67*, 26442. DOI: https://doi.org/10.3402/tellusb.v67.26442.

Fan, J., Leung, L. R., Rosenfeld, D., Chen, Q., Li, Z., Zhang, J., & Yan, H. (2013, Nov). Microphysical effects determine macrophysical response for aerosol impacts on deep convective clouds. *Proceedings of the National Academy of Sciences of the United States of America*, *110*(48), E4581–E4590. doi: 10.1073/pnas.1316830110

Fan, J., Rosenfeld, D., Zhang, Y., Giangrande, S. E., Li, Z., Machado, L. A. T., et al. (2018, Jan). Substantial convection and precipitation enhancements by ultrafine aerosol particles. *Science*, *359*(6374), 411–418. doi: 10.1126/science.aan8461

Fan, J., Wang, Y., Rosenfeld, D., & Liu, X. (2016, Nov). Review of aerosol–cloud interactions: Mechanisms, significance, and challenges. *Journal of the Atmospheric Sciences*, *73*(11), 4221–4252. doi: 10.1175/JAS-D-16-0037.1

Fan, J., Zhang, R., Li, G., & Tao, W.-K. (2007). Effects of aerosols and relative humidity on cumulus clouds. *Journal of Geophysical Research: Atmospheres*, *112*(D14). doi: https://doi.org/10.1029/2006JD008136

Federer, B., Waldvogel, A., Schmid, W. Schiesser, H. H., Hampel, F., Schweingrube, M., et al. (1986). Main results of Grossversuch IV. *Journal of Applied Meteorology*, *25*, 917–957.

Feingold, G., Boers, R., Stevens, B., & Cotton, W. R. (1997). A modeling study of the effect of drizzle on cloud optical depth and susceptibility. *Journal of Geophysical Research*, *102*(D12), 13527–13534.

Feingold, G., Jiang, H., & Harrington, J. Y. (2005, Jan). On smoke suppression of clouds in Amazonia. *Geophysical Research Letters*, *32*(2), L02804. doi: 10.1029/ 2004GL021369

Fernando, H. J. S., Gultepe, I., Dorman, C., Pardyjak, E., Wang, Q., Hoch, S. W., et al. (2021, Feb). C-FOG: Life of coastal fog. *Bulletin of the American Meteorological Society*, *102*(2), E244–E272. doi: 10.1175/BAMS-D-19-0070.1

Field, P. R., & Wood, R. (2007, Jan). Precipitation and cloud structure in midlatitude cyclones. *Journal of Climate*, *20*(2), 233–254. doi: 10.1175/jcli3998.1

Findeisen W. (1938). Die kolloidmeteorologischen Vorgänge bei der Niederschlagsbildung (colloidal meteorological processes in the formation of precipitation). *Meteorologische Zeitschrift*, *55*, 121–133.

Flossmann, A. I., Manton, M., Abshaev, A., Bruintjes, R., Murakami, M., Prabhakaran T., & Yao, Z. (2019, Aug). Review of advances in precipitation enhancement research. *Bulletin of the American Meteorological Society*, *100*(8), 1465–1480. doi: 10.1175/BAMS-D-18-0160.1

Formenti, P., D'Anna, B., Flamant, C., Mallet, M., Piketh, S. J., Schepanski, K., et al. (2019, Jul). The aerosols, radiation and clouds in southern Africa field campaign in amibia: Overview, illustrative observations, and way forward. *Bulletin of the American Meteorological Society*, *100*(7), 1277–1298. doi: 10.1175/BAMS-D-17-0278.1

French, J. R., Friedrich, K., Tessendorf, S. A., Rauber, R. M., Geerts, B., Rasmussen, R. M., et al. (2018, Jan). Precipitation formation from orographic cloud seeding. *Proceedings of the National Academy of Sciences*, *115*(6), 1168–1173.

Fridlind, A. M., Ackerman, A. S., Jensen, E. J., Heymsfield, A. J., Poellot, M. R., Stevens, D. E., et al. (2004, Apr). Evidence for the predominance of mid-tropospheric aerosols as subtropical anvil cloud nuclei. *Science*, *304*(5671), 718–722. doi: 10.1126/science.1094947

Garrett, T. J., Radke, L. F., & Hobbs, P. V. (2002, Feb). Aerosol effects on cloud emissivity and surface longwave heating in the Arctic. *Journal of the Atmospheric Sciences*, *59*(3), 769–778. doi: 10.1175/1520-0469(2002)059(0769:AEOCEA)2.0.CO;2

Gasparini, B., & Lohmann, U. (2016). Why cirrus cloud seeding cannot substantially cool the planet. *Journal of Geophysical Research: Atmospheres*, *121*(9), 4877–4893. doi: https://doi.org/10.1002/2015JD024666

Gassó, S. (2008). Sat llite observations of the impact of weak volcanic activity on marine clouds. *Journal of Geophysical Research: Atmospheres 113*(D14). doi: 10.1029/2007JD009106

Gautam, R., Hsu, N. C., Kafatos, M., & Tsay, S.-C. (2007). Influences of winter haze on fog/low cloud over the Indo-Gangetic plains. *Journal of Geophysical Research: Atmospheres*, *112*(D5). doi: https://doi.org/10.1029/2005JD007036

Gettelman, A., Bardeen, C. G., McCluskey, C. S., Järvinen, E., Stith, J., Bretherton, C., et al. (2020). Simulating observations of Southern Ocean clouds and implications for climate. *Journal of Geophysical Research: Atmospheres*, *125*(21), e2020JD032619. doi: https://doi.org/10.1029/2020JD032619

Gettelman, A., Lin, L., Medeiros, B., & Olson, J. (2016, Sep). Climate feedback variance and the interaction of aerosol forcing and feedbacks. *Journal of Climate*, *29*(18), 6659–6675. doi: 10.1175/JCLI-D-16-0151.1

Gettelman, A., Liu, X., Barahona, D., Lohmann, U., & Chen, C. (2012). Climate impacts of ice nucleation. *Journal of Geophysical Research Atmospheres*, *117*(20), 1–14. doi: 10.1029/2012JD017950

Ghan, S. J., Abdul-Razzak, H., enes, A., Ming, Y., Liu, X., Ovchinnikov, M., et al. (2011, Apr). Droplet nucleation: Physically-based parameterizations and comparative evaluation. *Journal of Advances in Modeling Earth Systems*, *3*(4). doi: 10.1029/2011ms000074

Ghude, S. D., Bhat, G., Prabhakaran, T., Jenamani, R., Chate, D., Safai, P., et al. (2017). Winter fog experiment over the Indo-Gangetic plains of India. *Current Science*, 767–784.

Givati, A., & Rosenfeld, D. (2004, Jul). Quantifying precipitation suppression due to air pollution. *Journal of Applied Meteorology*, *43*(7), 1038–1056. doi: 10.1175/1520-0450(2004)043⟨1038:QPSDTA⟩2.0.CO;2

Glassmeier, F., Hoffmann, F., Johnson, J. S., Yamaguchi, T., Carslaw, K. S., & Feingold, G. (2019). An emulator approach to statocumulus susceptibility. *Atmospheric Chemistry and Physics*, *19*, 10191–10203.

Glassmeier, F., Hoffmann, F., Johnson, J. S., Yamaguchi, T., Carslaw, K. S., & Feingold, G. (2021). Aerosol-cloud-climate cooling overestimated by ship-track data. *Science*, *371*, 485–489.

Glassmeier, F., & Lohmann, U. (2016). Constraining precipitation susceptibility of warm, iceand mixed-phase clouds with microphysical equations. *Journal of the Atmospheric Sciences*, *73*(12), 5003–5023.

Glassmeier, F., & Lohmann, U. (2018). Precipitation susceptibility and aerosol buffering of warm and mixed-phase orographic clouds in idealized simulations. *Journal of the Atmospheric Sciences* *75*(4), 1173–1194.

Gordon, H., Field, P. R., Abel, S. J., Barrett, P., Bower, K., Crawford, I., et al. (2020, Sep). Development of aerosol activation in the double-moment Unified Model and evaluation with CLARIFY measurements. *Atmospheric Chemistry and Physics*, *20*(18), 10997–11024. doi: 10.5194/acp-20-10997-2020

Gordon, H., Field, P. R., Abel, S. J., Dalvi, M., Grosvenor, D. P., Hill, A. A., et al. (2018, Oct). Large simulated radiative effects of smoke in the south-east Atlantic. *Atmospheric Chemistry and Physics*, *18*(20) 15261–15289. doi: 10.5194/acp-18-15261-2018

Goren, T., & Rosenfeld, D. (2012). Satellite observations of ship emission induced transitions from broken to closed cell marine stratocumulus over large areas. *Journal of Geophysical Research: Atmospheres*, *117*(D17).

Goren, T., & Rosenfeld, D. (2014, Mar). Decomposing aerosol cloud radiative effects into cloud cover, liquid water path and Twomey components in marine stratocumulus. *Atmospheric Research*, *138*, 378–393. doi: 10.1016/j.atmosres.2013.12.008

Goren, T., & Rosenfeld, D. (2015). Extensive closed cell marine stratocumulus downwind of Europe–A large aerosol cloud mediated radiative effect or forcing? *Journal of Geophysical Research: Atmospheres*, *120*(12), 6098–6116.

Grabowski, W. W. (2018, Oct). Can the impact of aerosols on deep convection be isolated from meteorological effects in atmospheric observations? *Journal of the Atmospheric Sciences*, *75*(10), 3347–3363. doi: 10.1175/JAS-D-18-0105.1

Grabowski, W. W., & Morrison, H. (2016, Sep). Untangling microphysical impacts on deep convection applying a novel modeling methodology. Part II: Double-moment microphysics. *Journal of the Atmospheric Sciences*, *73*(99), 3749–3770. Retrieved from http://journals.ametsoc.org/doi/10.1175/JAS-D-15-0367.1. doi: 10.1175/JAS-D-15-0367.1

Grabowski, W. W., & Morrison, H. (2020). Do ultrafine cloud condensation nuclei invigorate deep convection? *Journal of the Atmospheric Sciences*, *77*(7), 2567–2583. doi: 10.1175/JAS-D-20-0012.1

Graf, M. A., Wernli, H., & Sprenger, M. (2017). Objective classification of extratropical cyclogenesis. *Quarterly Journal of the Royal Meteorological Society*, *143*(703), 1047–1061.

Grandey, B. S., Stier, P., Grainger, R. G., & Wagner, T. M. (2013). The contribution of the strength and structure of extratropical cyclones to observed cloudaerosol relationships. *Atmospheric Chemistry and Physics*, *13*(21), 10689–10701. doi: 10.5194/acp-13-10689-2013

Grandey, B. S., Stier, P., & Wagner, T. M. (2013). Investigating relationships between aerosol optical depth and cloud fraction using satellite, aerosol reanalysis and general circulation model data. *Atmospheric Chemistry and Physics*, *13*(6), 3177–3184. doi: 10.5194/acp-13-3177-2013

Grosvenor, D. P., Field, P. R., Hill, A. A., & Shipway, B. J. (2017). The relative importance of macrophysical and cloud albedo changes for aerosol-induced radiative effects in closed-cell stratocumulus: Insight from the modelling of a case study. *Atmospheric Chemistry and Physics*, *17*(8), 5155–5183.

Grosvenor, D. P., Sourdeval, O., Zuidema, P., Ackerman, A., Alexandrov, M. D., Bennartz, R., et al. (2018, Jun). Remote sensing of droplet number concentration in warm clouds: A review of the current state of knowledge and perspectives. *Reviews of Geophysics*, *56*(2), 409–453. doi: 10.1029/2017RG000593

Grosvenor, D. P., & Wood, R. (2014). The effect of solar zenith angle on MODIS cloud optical and microphysical retrievals within marine liquid water clouds. *Atmospheric Chemistry & Physics*, *14*(14), 7291–7321. doi: 10.5194/acp-14-7291-2014

Gryspeerdt, E. (2019). Ruskin and meteorology. In S. F. Cooper & R. Johns (Eds.), *Ruskin, turner and the storm cloud*. Paul Holberton Publishing.

Gryspeerdt, E., Goren, T., Sourdeval, O., Quaas, J., Mülmenstädt, J., Dipu, S., et al. (2019, Apr). Constraining the aerosol influence on cloud liquid water path. *Atmospheric Chemistry and Physics*, *19*(8), 5331–5347. doi: 10.5194/acp-19-5331-2019

Gryspeerdt, E., Mülmenstädt, J., Gettelman, A., Malavelle, F. F., Morrison, H., Neubauer, D., et al. (2018). Ice crystal number concentration estimates from lidar-radar satellite remote

sensing Part 2: Controls on the ice crystal number concentration. *Atmospheric Chemistry and Physics*, *18*, 14351–14370.

Gryspeerdt E., Mülmenstädt, J., Gettelman, A., Malavelle, F. F., Morrison, H., eubauer, D., et al. (2020). Surprising similarities in model and observational aerosol radiative forcing estimates. *Atmospheric Chemistry and Physics*, *20*(1), 613–623. doi: 10.5194/acp-20-613-2020

Gryspeerdt, E., Quaas, J., & Bellouin, . (2016). Constraining the aerosol influence on cloud fraction. *Journal of Geophysical Research: Atmospheres*, *121*(7). doi: 10.1002/2015JD023744

Gryspeerdt, E., Quaas, J., Ferrachat S., Gettelman, A., Ghan, S., Lohmann, U., et al. (2017, May). Constraining the instantaneous aerosol influence on cloud albedo. *Proceedings of the National Academy of Sciences*, *114*(19), 4899–4904. doi: 10.1073/pnas.1617765114

Gryspeerdt, E., Smith, T. W. P., O'Keeffe, E., Christensen, M. W., & Goldsworth, F. W. (2019, ov). The impact of ship emission controls recorded by cloud properties. *Geophysical Research Letters*, *46*, 12,547–12,555. https://doi.org/10.1029/2019GL084700

Gryspeerdt, E., Sourdeval, O., Quaas, J., Delanoë, J., Krämer, M., & Kühne, P. (2018, Oct). Ice crystal number concentration estimates from lidarradar satellite remote sensing – Part 2: Controls on the ice crystal number concentration. *Atmospheric Chemistry and Physics* *18*(19), 14351–14370. Retrieved from https://acp.copernicus.org/articles/18/14351/2018/ doi: 10.5194/acp-18-14351-2018

Gryspeerdt, E., & Stier, P. (2012). Regime-based analysis of aerosol-cloud interactions. *Geophysical Research Letters*, *39*(21). doi: https://doi.org/10.1029/2012GL053221

Hamilton, D. S., Lee, L. A., Pringle, K. J., Reddington, C. L., Spracklen, D. V., & Carslaw, K. S. (2014). Occurrence of pristine aerosol environments on a polluted planet. *Proceedings of the National Academy of Sciences*, *111*(52), 18466–18471. doi: 10.1073/pnas.1415440111

Hansen, J., Sato, M., Kharecha, P., & von Schuckmann, K. (2011). Earth's energy imbalance and implications. *Atmospheric Chemistry and Physics*, *11*(24), 13421–13449. doi: 10.5194/acp-11-13421-2011

Hansen, J., Sato, M., & Ruedy, R. (1997, Mar). Radiative forcing and climate response. *Journal of Geophysical Research Atmospheres*, *102*(D6), 6831–6864. doi: 10.1029/96JD03436

Hasekamp, O. P., Gryspeerdt, E., & Quaas, J. (2019, Nov). Analysis of po-larimetric satellite measurements suggests stronger cooling due to aerosol-cloud interactions. *Nature Communications*, *10*(1), 5405.

Haywood, J. M., Abel, S. J., Barrett, P. A., Bellouin, ., Blyth, A., Bower, K. N., et al. (2021). The cloud–aerosol–radiation interaction and forcing: Year 2017 (CLARIFY-2017) measurement campaign. *Atmospheric Chemistry and Physics*, *21*(2), 1049–1084. doi: 10.5194/acp-21-1049-2021

Herbert, R. J., Bellouin, ., Highwood, E. J., & Hill, A. A. (2020, Feb). Diurnal cycle of the semi-direct effect from a persistent absorbing aerosol layer over marine stratocumulus in large-eddy simulations. *Atmospheric Chemistry and Physics*, *20*(3), 1317–1340. doi: 10.5194/acp-20-1317-2020

Heyn, I., Block, K., Mülmenstädt, J., Gryspeerdt, E., Kühne, P., Salzmann, M., & Quaas, J. (2017). Assessment of simulated aerosol effective radiative forcings in the terrestrial spectrum. *Geophysical Research Letters*, *44*(2), 1001–1007. doi: https://doi.org/10.1002/2016GL071975

Hilario, M. R. A., Crosbie, E., Shook, M., Reid, J. S., Cambaliza, M. O. L., Simpas, J. B. B., et al. (2021). Measurement report: Long-range transport patterns into the tropical northwest Pacific during the CAMP^{2}Ex aircraft campaign: Chemical composition, size distributions, and the impact of convection. *Atmospheric Chemistry and Physics*, *21*(5), 3777–3802. doi: 10.5194/acp-21-3777-2021

Hill, A. A., Feingold, G., & Jiang, H. (2009, May). The influence of entrainment and mixing assumption on aerosol-cloud interactions in marine stratocumulus. *Journal of the Atmospheric Sciences*, *66*(5), 1450–1464. doi: 10.1175/2008JAS2909.1

Hobbs, P. V., Garrett, T. J., Ferek, R. J., Strader, S. R., Hegg, D. A., Frick, G. M., et al. (2000, Aug). Emissions from ships with respect to their effects on clouds. *Journal of the Atmospheric Sciences*, *57*(16), 2570–2590. doi: 10.1175/1520-0469(2000)057⟨2570: EFSWRT⟩2.0.CO;2

Hoffmann, F., & Feingold, G. (2019). Entrainment and mixing in stratocumulus: Effects of a new explicit subgrid-scale scheme for large-eddy simulations with particle-based microphysics. *Journal of the Atmospheric Sciences*, *76*(7), 1955–1973.

Hu, Y., Vaughan, M., McClain, C., Behrenfeld, M., Maring, H., Anderson, D., et al. (2007). Global statistics of liquid water content and effective number concentration of water clouds over ocean derived from combined CALIPSO and MODIS measurements. *Atmospheric Chemistry and Physics*, *7*(12), 3353–3359. doi: 10.5194/acp-7-3353-2007

Hu, Y. X., Rodier, S., Xu, K. M., Sun, W. B., Huang, J. P., Lin, B., et al. (2010, Oct). Occurrence, liquid water content, and fraction of supercooled water clouds from combined CALIOP/IIR/MODIS measurements. *Journal of Geophysical Research-Atmospheres*, *115*, 13. doi: 10.1029/2009jd012384

Hudson, J. G., & Squires, P. (1976, Jul). Improved continuous flow diffusion cloud chamber. *Journal of Applied Meteorology*, *15*(7), 776–782. doi: 10.1175/1520-0450(1976)015⟨0776:AICFDC⟩2.0.CO;2

Igel, A. L., & van den Heever S. C. (2021). Invigoration or enervation of convective clouds by aerosols? *Geophysical Research Letters*, *48*(16), e2021GL093804. doi: https://doi.org/10.1029/2021GL093804

Jensen, E. J., & Toon, O. B. (1992). The potential effects of volcanic aerosols on cirrus cloud microphysics. *Geophysical Research Letters*, *19*(17), 1759–1762. doi: https://doi.org/10.1029/92GL01936

Jensen, J. B., & Nugent, A. D. (2017, Mar). Condensational growth of drops formed on giant sea-salt aerosol particles. *Journal of the Atmospheric Sciences*, *74*(3), 679–697. doi: 10.1175/JAS-D-15-0370.1

Jiang, J. H., Su, H., Zhai, C., Perun, V. S., Del Genio, A., Nazarenko, L. S., et al. (2012). Evaluation of cloud and water vapor simulations in CMIP5 climate models using ASA "A-Train" satellite observations. *Journal of Geophysical Research: Atmospheres*, *117*(D14), D14105. doi: 10.1029/2011JD017237

Johnson, B. T. (2005 Jul). Large-eddy simulations of the semidirect aerosol effect in shallow cumulus regimes. *Journal*

of Geophysical Research: Atmospheres, *110*(D14). doi: 10.1029/2004JD005601

Johnson, B. T., Shine, K. P., & Forster P. M. (2004, Apr). The semi-direct aerosol effect: Impact of absorbing aerosols on marine stratocumulus. *Quarterly Journal of the Royal Meteorological Society*, *130*(599 PART B), 1407–1422. doi: 10.1256/ qj.03.61

Johnson, D. B. (1982, Feb). The role of giant and ultra-giant aerosol particles in warm rain initiation. *Journal of Atmospheric Sciences*, *39*(2), 448–460. doi: 10.1175/1520-0469(1982)039⟨0448:TROGAU⟩2.0.CO;2

Johnson, J. S., Cui, Z., Lee, L. A., Gosling, J. P., Blyth, A. M., & Carslaw, K. S. (2015). Evaluating uncertainty in convective cloud microphysics using statistical emulation. *Journal of Advances in Modeling Earth Systems*, *7*(1), 162–187. doi: https://doi.org/10.1002/2014MS000383

Johnson, J. S., Regayre, L. A., Yoshioka, M., Pringle, K. J., Turnock, S. T., Browse, J., et al. (2020). Robust observational constraint of uncertain aerosol processes and emissions in a climate model and the effect on aerosol radiative forcing. *Atmospheric Chemistry and Physics*, *20*(15), 9491–9524. doi: 10.5194/acp-20-9491-2020

Kanji, Z. A., Ladino, L. A., Wex, H., Boose, Y., Burkert-Kohn, M., Cziczo, D. J., & Krämer, M. (2017, Jan). Overview of ice nucleating particles. *Meteorological Monographs*, *58*, 1.1–1.33. doi: 10.1175/ AMSMO OGRAPHS-D-16-0006.1

Kärcher, B. & Lohmann, U. (2002). A parameterization of cirrus cloud formation: Homogeneous freezing including effects of aerosol size. *Journal of Geophysical Research: Atmospheres*, *107*(D23), AAC 9-1–AAC 9-10. doi: https://doi.org/10.1029/2001JD001429

Kärcher, B. & Lohmann, U. (2003). A parameterization of cirrus cloud formation: Heterogeneous freezing. *Journal of Geophysical Research: Atmospheres*, *108*(D14). doi: https://doi.org/10.1029/2002JD003220

Kazil, J., Wang, H., Feingold, G., Clarke, A. D., Snider, J. R., & Bandy, A. R. (2011, Aug). Modeling chemical and aerosol processes in the transition from closed to open cells during VOCALS-REx. *Atmospheric Chemistry and Physics*, *11*(15), 7491–7514. doi: 10.5194/acp-11-7491-2011

Khain, A., Ovtchinnikov, M., Pinsky, M. Pokrovsky, A., & Krugliak, H. (2000, Dec). Notes on the state-of-the-art numerical modeling of cloud microphysics. *Atmospheric Research*, *55*(3–4), 159–224. doi: 10.1016/S0169-8095(00)00064-8

Khain, A., Pokrovsky, A., Pinsky, M., Seifert, A., & Phillips, V. (2004 Dec). Simulation of effects of atmospheric aerosols on deep turbulent convective clouds using a spectral microphysics mixed-phase cumulus cloud model. Part I: Model description and possible applications. *Journal of the Atmospheric Sciences*, *61*(24), 2963–2982. doi: 10.1175/JAS-3350.1

Khairoutdinov, M., & Kogan, Y. (2000, Jan). A new cloud physics parameterization in a large-eddy simulation model of marine stratocumulus. *Monthly Weather Review*, *128*(1), 229–243. doi: 10.1175/1520-0493(2000)128⟨0229:ANCPPI⟩2.0.CO;2

Knollenberg, R. G. (1976). *Three New Instruments for Cloud Physics Measurements: The 2-D Spectrometer, the Forward Scattering Spectrometer Probe, and the Active Scattering Aerosol Spectrometer*. In *Preprints, International Conference on Cloud Physics* (pp. 554–561). American Meteorological Society.

Knutti, R., Furrer, R., Tebaldi, C., Cermak, J., & Meehl G. A. (2010, May). Challenges in combining projections from multiple climate models. *Journal of Climate*, *23*(10), 2739–2758. doi: 10.1175/2009JCLI3361.1

Koch, D., & Del Genio, A. D. (2010, Aug). Black carbon semi-direct effects on cloud cover: Review and synthesis. *Atmospheric Chemistry and Physics*, *10*(16), 7685–7696. doi: 10.5194/acp-10-7685-2010

Köhler, H. (1936, Jan). The nucleus in and the growth of hygroscopic droplets. *Transactions of the Faraday Society*, *32*, 1152–1161. doi: 10.1039/ TF9363201152

Kollias, P., Bharadwaj, N., Clothiaux, E. E., Lamer, K., Oue, M., Hardin, J., et al. (2020, May). The arm radar network: At the leading edge of cloud and precipitation observations. *Bulletin of the American Meteorological Society*, *101*(5), E588–E607. doi: 10.1175/BAMS-D-18-0288.1

Koren, I., Dagan, G., & Altaratz, O. (2014). From aerosol-limited to invigoration of warm convective clouds. *Science*, *344*(6188), 1143–1146. doi: 10.1126/science.1252595

Koren, I., Kaufman, Y. J., Remer, L. A., & Martins, J. V. (2004). Measurement of the effect of Amazon smoke on inhibition of cloud formation. *Science*, *303*(5662), 1342–1345. doi: 10.1126/science.1089424

Korolev, A. V., & Mazin, I. P. (2003). Supersaturation of water vapor in clouds. *Journal of the Atmospheric Sciences*, *60*(24), 2957–2974. doi: 10.1175/1520-0469(2003)060⟨2957:SOWVIC⟩2.0.CO;2

Krasnopolsky, V. M., Fox-Rabinovitz, M. S., & Chalikov, D. V. (2005, May). New approach to calculation of atmospheric model physics: Accurate and fast neural network emulation of longwave radiation in a climate model. *Monthly Weather Review*, *133*(5), 1370–1383. doi: 10.1175/MWR2923.1

Kreidenweis, S. M., Petters, M., & Lohmann, U. (2019, Jan). 100 years of progress in cloud physics, aerosols, and aerosol chemistry research. *Meteorological Monographs*, *59*, 11.1–11.72. doi: 10.1175/amsmonographs-d-18-0024.1

Kulkarni, P., & Wang, J. (2006, Oct). New fast integrated mobility spectrometer for real-time measurement of aerosol size distribution-I: Concept and theory. *Journal of Aerosol Science*, *37*(10), 1303–1325. doi: 10.1016/j.jaerosci.2006.01.005

Lacis, A. A., & Hansen, J. E. (1974). A parameterization for the absorption of solar radiation in the Earth's atmosphere. *Journal of the Atmospheric Sciences*, *31*, 118–133.

Langmuir, I. (1950). Control of precipitation from cumulus clouds by various seeding techniques. *Science*, *112*(2898), 35–41.

Latham, J. (2002). Amelioration of global warming by controlled enhancement of the albedo and longevity of low-level maritime clouds. *Atmospheric Science Letters*, *3*(24), 52–58. doi: https://doi.org/10.1006/asle.2002.0099

Latham, J., Bower, K., Choularton, T., Coe, H., Connolly, P., Cooper, G., et al. (2012). Marine cloud brightening. *Philosophical Transactions of the Royal Society A: Mathematical, Physical and Engineering Sciences*, *370*(1974), 4217–4262. doi: 10.1098/rsta.2012.0086

L'Ecuyer, T. S., Hang, Y., Matus, A. V., & Wang, Z. (2019). Reassessing the effect of cloud type on Earth's energy balance in the age of active spaceborne observations. Part I: Top of atmosphere and surface. *Journal of Climate*, *32*(19), 6197–6217.

Lee, L. A., rslaw, K. S., Pringle, K. J., Mann, G. W., & Spracklen, D. V. (2011). Emulation of a complex global aerosol model to quantify sensitivity to uncertain parameters. *Atmospheric Chemistry and Physics*, *11*(23), 12253–12273.

Lee, L. A., Reddington, C. L., & Carslaw, K. S. (2016, May). On the relationship between aerosol model uncertainty and radiative forcing uncertainty. *Proceedings of the National Academy of Sciences*, *113*(21), 5820–5827. doi: 10.1073/pnas.1507050113

Li J., Jian, B., Huang, J., Hu, Y., Zhao, C., Kawamoto, K., et al. (2018, Aug). Long-term variation of cloud droplet number concentrations from space-based Lidar. *Remote Sensing of Environment*, *213*, 144–161. doi: https://doi.org/10.1016/j.rse.2018.05.011

Liu, B. Y., Whitby, K. T., & Pui, D. Y. (1974). A portable electrical analyzer for size distribution measurement of submicron aerosols. *Journal of the Air Pollution Control Association*, *24*(11), 1067–1072. doi: 10.1080/ 00022470.1974.10470016

Liu, L., Cheng, Y., Wang, S., Wei, C., Pöhlker, M. L., Pöhlker, C., et al. (2020). Impact of biomass burning aerosols on radiation, clouds, and precipitation over the Amazon: Relative importance of aerosol–cloud and aerosol–radiation interactions. *Atmospheric Chemistry and Physics*, *20*(21), 13283–13301. doi: 10.5194/acp-20-13283-2020

Liu, Y., Zhang, K., Qian, Y., Wang, Y., Zou, Y., Song, Y., et al. (2018). Investigation of short-term effective radiative forcing of fire aerosols over orth America using nudged hindcast ensembles. *Atmospheric Chemistry and Physics*, *18*(1), 31–47. doi: 10.5194/acp-18-31-2018

Lohmann, U., & Ferrachat, S. (2010). Impact of parametric uncertainties on the present-day climate and on the anthropogenic aerosol effect. *Atmospheric Chemistry and Physics*, *10*(23), 11373–11383. doi: 10.5194/acp-10-11373-2010

Lohmann, U., & Gasparini, B. (2017). A cirrus cloud climate dial? *Science*, *357*(6348).

Lohmann, U., Spichtinger, P., Jess, S., Peter, T., & Smit H. (2008, Oct). Cirrus cloud formation and ice supersaturated regions in a global climate model. *Environmental Research Letters*, *3*(4), 045022. doi: 10.1088/1748-9326/3/4/045022

Lu, Z., Liu, X., Zhang, Z., Zhao, C., Meyer, K., Rajapakshe, C., et al. (2018). Biomass smoke from Southern Africa can significantly enhance the brightness of stratocumulus over the Southeastern Atlantic ocean. *Proceedings of the National Academy of Sciences*, *115*(12), 2924–2929. doi: 10.1073/pnas.1713703115

Ma, P.-L., Rasch, P. J., Chepfer, H., Winker, D. M., & Ghan, S. J. (2018, Jul). Observational constraint on cloud susceptibility weakened by aerosol retrieval limitations. *Nature Communications*, *9*, 2640. doi: 10.1038/s41467-018-05028-4

Ma, Y., Ye, J., Xin, J., Zhang, W., Vil-Guerau de Arellano, J., Wang, S., et al. (2020). The stove, dome, and umbrella effects of atmospheric aerosol on the development of the planetary boundary layer in hazy regions. *Geophysical Research Letters*, *47*(13), e2020GL087373. doi: https://doi.org/10.1029/2020GL087373

Mace, G. G., & Abernathy, A. C. (2016). Observational evidence for aerosol invigoration in shallow cumulus downstream of Mount Kilauea. *Geophysical Research Letters*, *43*(6), 2981–2988. doi: 10.1002/2016GL067830

Mahajan, S., Evans, K. J., Truesdale, J. E., Hack, J. J., & Lamarque, J.-F. (2012, Dec). Interannual tropospheric aerosol variability in the late twentieth century and its impact on tropical Atlantic and west African climate by direct and semidirect effects. *Journal of Climate*, *25*(23), 8031–8056. doi: 10.1175/JCLI-D-12-00029.1

Malavelle F. F., Haywood, J. M., Mercado, L. M., Folberth, G. A., Bellouin, ., Sitch, S., & Artaxo, P. (2019, Jan). Studying the impact of biomass burning aerosol radiative and climate effects on the Amazon rainforest productivity with an Earth system model. *Atmospheric Chemistry and Physics*, *19*(2), 1301–1326. doi: 10.5194/acp-19-1301-2019

Mallet, M., abat, P., Zuidema, P., Redemann, J., Sayer, A. M., Stengel, M., et al. (2019, Apr). Simulation of the transport, vertical distribution, optical properties and radiative impact of smoke aerosols with the ALADI regional climate model during the ORACLES-2016 and LASIC experiments. *Atmospheric Chemistry and Physics*, *19*(7) 4963–4990. doi: 10.5194/acp-19-4963-2019

Manaster, A., O'Dell, C. W., & Elsaesser, G. (2017). Evaluation of cloud liquid water path trends using a multidecadal record of passive microwave observations. *Journal of Climate*, *30*(15), 5871–5884. doi: 10.1175/jcli-d-16-0399.1

Mann, J. A. L., Christine Chiu, J., Hogan, R. J., O'Connor, E. J., L'Ecuyer T. S., Stein, T. H. M., & Jefferson, A. (2014). Aerosol impacts on drizzle properties in warm clouds from ARM Mobile Facility maritime and continental deployments. *Journal of Geophysical Research: Atmospheres*, *119*(7), 4136–4148. doi: https://doi.org/10.1002/2013JD021339

Mann, M. E., Rahmstorf, S. Kornhuber, K., Steinman, B. A., Miller, S. K., Petri, S., & Coumou D. (2018). Projected changes in persistent extreme summer weather events: The role of quasi-resonant amplification. *Science Advances*, *4*(10). doi: 10.1126/sciadv.aat3272

Mason, B. J. (1960, Jan). ucleation of water aerosols. *Discussions of the Faraday Society*, *30*, 20–38. doi: 10.1039/DF9603000020

Mather, J. H., & Voyles J. W. (2013, Mar). The ARM climate research facility: A review of structure and capabilities. *Bulletin of the American Meteorological Society 94*(3), 377–392. doi: 10.1175/BAMS-D-11-00218.1

Mauger, G. S., & Norris, J. R. (2007). Meteorological bias in satellite estimates of aerosol-cloud relationships. *Geophysical Research Letters*, *34*(16). doi: 10.1029/ 2007gl029952

Mazoyer, M., Burnet, F., Denjean, C., Roberts G. C., Haeffelin M., Dupont, J.-C., & Elias, T. (2019). Experimental study of the aerosol impact on fog microphysics. *Atmospheric Chemistry and Physics*, *19*(7), 4323–4344. doi: 10.5194/acp-19-4323-2019

McComiskey, A., & Feingold, G. (2012). The scale problem in quantifying aerosol cloud indirect effects. *Atmospheric Chemistry and Physics*, *12*, 1031–1049.

McComiskey, A., Feingold, G., Frisch A. S., Turner, D. D., Miller, M. A., Chiu, J. C., et al. (2009). An assessment of aerosol-cloud interaction in marine stratus clouds based on surface remote sensing. *Journal of Geophysical Research 114*(D09203).

McCoy, D. T., Bender, F. A.-M., Mohrmann, J. K. C., Hartmann, D. L., Wood, R., & Grosvenor, D. P. (2017, Feb). The global aerosol-cloud first indirect effect estimated using MODIS, MERRA, and AeroCom. *Journal of Geophysical Research: Atmospheres*, *122*(3), 1779–1796. doi: 10.1002/2016JD026141

McCoy, D. T., Field, P., Gordon, H., Elsaesser, G. S., & Grosvenor, D. P. (2020). Untangling causality in midlatitude aerosolcloud adjustments. *Atmospheric Chemistry and Physics*, *20*(7), 4085–4103. doi: 10.5194/acp-20-4085-2020

McCoy, D. T., Field, P. R., Schmidt, A., Grosvenor, D. P., Bender, F. A. M., Ship-way, B. J., et al. (2018, Apr). Aerosol midlatitude cyclone indirect effects in observations and high-resolution simulations. *Atmospheric Chemistry and Physics*, *18*(8), 5821–5846. doi: 10.5194/acp-18-5821-2018

McCoy, D. T., & Hartmann, D. L. (2015). Observations of a substantial cloud-aerosol indirect effect during the 2014-2015 Bardabunga-Veidivotn fissure eruption in Iceland. *Geophysical Research Letters*, *42*(23), 10,409–10,414. doi: 10.1002/2015gl067070

McCoy, I. L., Bretherton, C. S., Wood, R., Twohy, C. H., Gettelman, A., Bardeen, C. G., & Toohey, D. W. (2021). Influences of recent particle formation on southern ocean aerosol variability and low cloud properties. *Journal of Geo-physical Research: Atmospheres*, *126*(8), e2020JD033529. doi: https://doi.org/10.1029/2020JD033529

McCoy, I. L., McCoy, D. T., Wood, R., Regayre, L., Watson-Parris, D., Grosvenor, D. P., et al. (2020). The hemispheric contrast in cloud microphysical properties constrains aerosol forcing. *Proceedings of the National Academy of Sciences*, *117*(32), 18998–19006. doi: 10.1073/pnas.1922502117

McCoy, I. L., Wood, R., & Fletcher, J. K. (2017). Identifying meteorological controls on open and closed mesoscale cellular convection associated with marine cold air outbreaks. *Journal of Geophysical Research: Atmospheres*, *122*(21), 11,678–11,702. doi: 10.1002/2017JD027031

McFarquhar, G. M., Bretherton, C., Marchand, R., Protat, A., DeMott, P. J., Alexander, S. P., et al. (2020, Nov). Observations of clouds, aerosols, precipitation, and surface radiation over the southern ocean: An overview of capricorn, marcus, micre and socrates. *Bulletin of the American Meteorological Society*, 1–92. doi: 10.1175/BAMS-D-20-0132.1

McFarquhar, G. M., & Wang, H. (2006, Apr). Effects of aerosols on trade wind cumuli over the Indian Ocean: Model simulations. *Quarterly Journal of the Royal Meteorological Society*, *132*(616), 821–843. doi: 10.1256/qj.04.179

Menon, S., Hansen, J., Nazarenko, L., & Luo, Y. (2002). Climate effects of black carbon aerosols in China and India. *Science*, *297*(5590), 2250–2253. doi: 10.1126/ science.1075159

Michibata, T., & Suzuki, K. (2020, Jun). Reconciling compensating errors between precipitation constraints and the energy budget in a climate model. *Geophysical Research Letters*, *47*(12), e2020GL088340. doi: 10.1029/2020GL088340

Miltenberger, A. K., Field, P. R., Hill, A. A., Shipway, B. J., & Wilkinson, J. M. (2018, Jul). Aerosolcloud interactions in mixed-phase convective clouds. Part 2: Meteorological ensemble. *Atmospheric Chemistry and Physics*, *18*(14), 10593–10613. doi: 10.5194/acp-18-10593-2018

Mitchell, D. L., & Finnegan, W. (2009). Modification of cirrus clouds to reduce global warming. *Environmental Research Letters*, *4*, 045102.

Morrison, H., & Grabowski, W. W. (2011). Cloud-system resolving model simulations of aerosol indirect effects on tropical deep convection and its thermodynamic environment. *Atmospheric Chemistry and Physics*, *11*, 10503–10523.

Morrison, H., & Grabowski, W. W. (2013). Response of tropical deep convection to localized heating perturbations: Implications for aerosol-induced convective invigoration. *Journal of the Atmospheric Sciences*. *70*(11), 3533–3555.

Muhlbauer, A., McCoy, I. L., & Wood, R. (2014). Climatology of stratocumulus cloud morphologies: Microphysical properties and radiative effects. *Atmospheric Chemistry and Physics*, *14*(13), 6695–6716. doi: 10.5194/acp-14-6695-2014

Mülmenstädt, J., am, C., Salzman, M., Kretzschmar, J., L'Ecuyer, T. S., Lohmann, U., et al. (2020). Reducing the aerosol forcing uncertainty using observational constraints on warm rain processes. *Science Advances*, *6*(eaaz6433).

Mülmenstädt, J. & Feingold, G. (2018). The radiative forcing of aerosol–cloud interactions in liquid clouds: Wrestling and embracing uncertainty. *Current Climate Change Reports*, *4*(1), 23–40. (This article is part of the Topical Collection on Aerosols and Climate) doi: 10.1007/s40641-018-0089-y

Murray, B. J., Carslaw, K. S., & Field, P. R. (2021). Opinion: Cloud-phase climate feedback and the importance of ice-nucleating particles. *Atmospheric Chemistry and Physics*, *21*(2), 665–679. doi: 10.5194/acp-21-665-2021

Murray, B. J., O'Sullivan, D., Atkinson, J. D., & Webb, M. E. (2012). Ice nucleation by particles immersed in supercooled cloud droplets. *Chemical Society Reviews*, *41*, 6519–6554. doi: 10.1039/ C2CS35200A

Nakajima, T., Higurashi, A., Kawamoto, K., & Penner, J. E. (2001). A possible correlation between satellite-derived cloud and aerosol microphysical parameters. *Geophysical Research Letters*, *28*(7), 1171–1174. doi: 10.1029/2000GL012186

ational Academies of Sciences, Engineering and Medicine. (2021). *Reflecting sunlight: Recommendations for solar geoengineering research and research governance*. Washington, DC: The ational Academies Press. doi: 10.17226/25762

Naud, C. M., Del Genio, A. D., Bauer, M., & Kovari, W. (2010, Jun). Cloud vertical distribution across warm and cold fronts in CloudSat-CALIPSO data and a general circulation model. *Journal of Climate*, *23*(12), 3397–3415. doi: 10.1175/2010jcli3282.1

Naud, C. M., Posselt, D. J., & van den Heever, S. C. (2017). Observed covariations of aerosol optical depth and cloud cover in extratropical cyclones. *Journal of Geophysical Research: Atmospheres*, *122*(19), 10,338–10,356. doi: 10.1002/2017JD027240

Norris, J. R., Allen, R. J., Evan, A. T., Zelinka, M. D., O'Dell, C. W., & Klein, S. A. (2016). Evidence for climate change in the satellite cloud record. *Nature*, *536*(7614), 72–75. doi: 10.1038/nature18273

Panicker, A., Pandithurai, G., Safai, P., Dipu, S., Prabha, T., & Konwar M. (2014). Observations of black carbon induced semi direct effect over North-East India. *Atmospheric Environment*, *98*, 685–692. doi: https://doi.org/10.1016/j.atmosenv.2014.09.034

Penner, J. E., Chen, Y., Wang, M., & Liu, X. (2009). Possible influence of anthropogenic aerosols on cirrus clouds and anthropogenic forcing. *Atmospheric Chemistry and Physics*, *9*(3), 879–896. doi: 10.5194/acp-9-879-2009

Penner, J. E., Zhou, C., & Liu, X. (2015). Can cirrus cloud seeding be used for geoengineering? *Geophysical Research Letters*, *42*, 8775–8782.

Petters, M. D., & Kreidenweis, S. M. (2007, Apr). A single parameter representation of hygroscopic growth and cloud condensation nucleus activity. *Atmospheric Chemistry and Physics*, *7*(8), 1961–1971. doi: 10.5194/acp-7-1961-2007

Petters M. D., & Kreidenweis, S. M. (2013, Jan). A single parameter representation of hygroscopic growth and cloud condensation nucleus activity. Part 3: Including surfactant partitioning. *Atmospheric Chemistry and Physics*, *13*(2), 1081–1091. doi: 10.5194/acp-13-1081-2013

Petty, G. (2006). *A first course in atmospheric radiation*. Sundog Publishing.

Platnick, S. King, M. D., Ackerman, S. A., Menzel, W. P., Baum, B. A., Riedi, J. C., & Frey, R. A. (2003, Feb). The MODIS cloud products: Algorithms and examples from Terra. *IEEE Transactions on Geoscience and Remote Sensing*, *41*(2), 459–473. doi: 10.1109/tgrs.2002.808301

Platnick, S., & Twomey, S. (1994). Determining the susceptibility of cloud albedo to changes in droplet concentration with the advanced very high re olution radiometer. *Journal of Applied Meteorology*, *33*, 334–347.

Poku, C., Ross, A. N., Hill, A. A., Blyth, A. M., & Shipway, B. (2021). Is a more physical representation of aerosol activation needed for simulations of fog? *Atmospheric Chemistry and Physics*, *21*(9), 7271–7292. doi: 10.5194/acp-21-7271-2021

Politovich, M. K., & Cooper, W. A. (1988). Variability of the supersaturation in cumulus clouds. *Journal of the Atmospheric Sciences*, *45*(11), 1651–1664. doi: 10.1175/1520-0469(1988)045(1651:VOTSIC)2.0.CO;2

Posselt, R. & Lohmann, U. (2008). Influence of Giant CCN on warm rain processes in the ECHAM5 GCM. *Atmospheric Chemistry and Physics*, *8*(14), 3769–3788. doi: 10.5194/acp-8-3769-2008

Possner, A., Wang, H., Wood, R., Caldeira, K., & Ackerman, T. P. (2018). The efficacy of aerosolcloud radiative perturbations from near-surface emissions in deep open-cell stratocumuli. *Atmospheric Chemistry and Physics*, *18*(23), 17475–17488.

Possner, A., Zubler, E., Lohmann, U., & Schär, C. (2016, May). The resolution dependence of cloud effects and ship-induced aerosol-cloud interactions in marine stratocumulus. *Journal of Geophysical Research: Atmospheres*, *121*(9), 4810–4829. doi: 10.1002/2015JD024685

Prabhakaran, P., Shawon, A. S. M., Kinney, G., Thomas, S., Cantrell, W., & Shaw, R. A. (2020, Jul). The role of turbulent fluctuations in aerosol activation and cloud formation. *Proceedings of the National Academy of Sciences of the United States of America*, *117*(29), 16831–16838. doi: 10.1073/pnas.2006426117

Prisle . L., Asmi A., Topping, D., Partanen, A.-I. Romakkaniemi, S., Dal Maso, M., et al. (2012, Mar). Surfactant effects in global simulations of cloud droplet activation. *Geophysical Research Letters*, *39*(5). doi: 10.1029/2011GL050467

Pruppacher, H., & Klett, J. (2010). Diffusion growth and evaporation of water drops and snow crystals. In *Microphysics of clouds and precipitation* (pp. 502–567). Dordrecht: Springer Netherlands. doi: 10.1007/978-0-306-48100-0 13

Qian, Y., Wan, H., Yang, B. Golaz, J.-C., Harrop, B., Hou, Z., et al. (2018, Dec). Parametric sensitivity and uncertainty quantification in the version 1 of E3SM atmosphere model based on short perturbed parameter ensemble simulations. *Journal of Geophysical Research: Atmospheres*, *123*(23), 13,046–13,073. doi: 10.1029/2018JD028927

Quaas, J., Arola, A., Cairns, B., Christensen, M., Deneke, H., Ekman, A. M. L., et al. (2020, Dec). Constraining the Twomey effect from satellite observations: Issues and perspectives. *Atmospheric Chemistry and Physics*, *20*(23), 15079–15099. doi: 10.5194/acp-20-15079-2020

Quaas, J., Ming, Y., Menon, S., Takemura, T., Wang, M., Penner, J. E., et al. (2009). Aerosol indirect effects general circulation model intercomparison and evaluation with satellite data. *Atmospheric Chemistr and Physics*, *9*(22) 8697–8717.

Rajapakshe, C., Zhang, Z. Yorks, J. E., Yu, H., Tan, Q., Meyer, K., et al. (2017, Jun). Seasonally transported aerosol layers over southeast Atlantic are closer to underlying clouds than previously reported. *Geophysical Research Letters*, *44*(11), 5818–5825. doi: 10.1002/2017GL073559

Rasmussen, C. E., & Williams, C. K. I. (2006). *Gaussian processes for machine learning*. London: MIT press.

Redemann, J., Wood, R., Zuidema, P., Doherty, S. J., Luna, B., LeBlanc, S. E., et al. (2021). An overview of the ORACLES (observations of aerosols above clouds and their interactions) project: Aerosol–cloud–radiation interactions in the southeast Atlantic basin. *Atmospheric Chemistry and Physics*, *21*(3), 1507–1563. doi: 10.5194/acp-21-1507-2021

Regayre, L., Schmale, J., Johnson, J., Tatzelt, C. Baccarini, A., Henning, S., et al. (2019). The value of remote marine aerosol measurements for constraining radiative forcing uncertainty. *Atmospheric Chemistry and Physics*, 1–11. doi: 10.5194/acp-2019-1085

Regayre, L. A., Johnson J. S., Yoshioka, M., Pringle, K. J., Sexton, D. M., Booth, B. B., et al. (2018, Jul). Aerosol and physical atmosphere model parameters are both important sources of uncertainty in aerosol ERF. *Atmospheric Chemistry and Physics 18*(13), 9975–10006. doi: 10.5194/acp-18-9975-2018

Rosenfeld, D., Andreae, M. O., Asmi A., Chin, M., de Leeuw, G., Donovan, D. P., et al. (2014, Dec). Global observations of aerosol-cloud-precipitation-climate interactions. *Reviews of Geophysics*, *52*(4), 750–808. doi: 10.1002/2013RG000441

Rosenfeld, D., Kaufman, Y., & Koren, I. (2006). Switching cloud cover and dynamical regimes from open to closed Benard cells in response to the suppression of precipitation by aerosols. *Atmospheric Chemistry and Physics*, *6*(9) 2503–2511.

Rosenfeld, D., Lohmann, U., Raga, G. B., O'Dowd, C. D., Kulmala, M., Fuzzi, S., et al. (2008, Sep). Flood or drought:

How do aerosols affect precipitation? *Science*, *321*(5894), 1309–1313. doi: 10.1126/science.1160606

Rosenfeld, D., Zhu, Y., Wang, M., Zheng, Y., Goren, T., & Yu, S. (2019, Feb). Aerosol-driven droplet concentrations dominate coverage and water of oceanic low-level clouds. *Science*, *363*(6427). doi: 10.1126/science.aav0566

Safai, P. D., Ghude, S., Pithani, P. Varpe, S., Kulkarni, R., Todekar, K., et al. (2019). Two-way relationship between aerosols and fog: A case study at IGI airport, New Delhi. *Aerosol and Air Quality Research*, *19*(1), 71–79. doi: 10.4209/aaqr.2017.11.0542

Sanchez, K. J., Chen, C.-L., Russell, L. M., Betha, R., Liu, J., Price, D. J., et al. {2018). Substantial seasonal contribution of observed biogenic sulfate particles to cloud condensation nuclei. *Scientific Reports*, *8*(1), 1–14.

Sato, Y., Miura, H., Yashiro, H., Goto, D., Takemura, T., Tomita, H., & Nakajima, T. (2016, May). Unrealistically pristine air in the Arctic produced by current global scale models. *Scientific Reports*, *6*, 26561. doi: 10.1038/srep26561

Schneider, T., Teixeira, J., Bretherton, C. S., Brient, F., Pressel, K. G., Schär, C., & Siebesma, A. P. (2017, Jan). Climate goals and computing the future of clouds. *Nature Climate Change*, *7*(1), 3–5. doi: 10.1038/nclimate3190

Schutgens, . A. J., Gryspeerdt, E., Weigum, ., Tsyro, S., Goto, D., Schulz, M., & Stier, P. (2016 May). Will a perfect model agree with perfect observations? The impact of spatial sampling. *Atmospheric Chemistry and Physics*, *16*(10), 6335–6353. doi: 10.5194/acp-16-6335-2016

Schwartz, S. E. (1988, Dec). Are global cloud albedo and climate controlled by marine phytoplankton? *Nature*, *336*(6198), 441–445. doi: 10.1038/336441a0

Schwenkel, J., & Maronga, B. (2019, May). Large-eddy simulation of radiation fog with comprehensive two-moment bulk microphysics: Impact of different aerosol activation and condensation parameterizations. *Atmospheric Chemistry and Physics*, *19*(10), 7165–7181. doi: 10.5194/acp-19-7165-2019

Seinfeld, J. H., Bretherton, C., Carslaw, K. S., Coe, H., DeMott, P. J., Dunlea, E. J., et al. (2016, May). Improving our fundamental understanding of the role of aerosol-cloud interactions in the climate system. *Proceedings of the National Academy of Sciences of the United States of America*, *113*(21), 5781–5790. doi: 10.1073/pnas.1514043113

Sexton, D. M. H., Murphy, J. M., Collins, M., & Webb, M. J. (2012, Jun). Multivariate probabilistic projections using imperfect climate models. Part I: Outline of methodology. *Climate Dynamics*, *38*(11–12), 2513–2542. doi: 10.1007/s00382-011-1208-9

Shaw, R. A., Cantrell, W., Chen, S., Chuang, P., Donahue, N., Feingold, G., et al. (2020, Jul). Cloud–aerosol–turbulence interactions: Science priorities and concepts for a large-scale laboratory facility. *Bulletin of the American Meteorological Society*, *101*(7), E1026–E1035. doi: 10.1175/BAMS-D-20-0009.1

Shindell, D., & Smith, C. J. (2019, Sep). Climate and air-quality benefits of a realistic phase-out of fossil fuels. *Nature*, *573*(7774), 408–411. doi: 10.1038/s41586-019-1554-z

Shinozuka, Y., Saide, P. E., Ferrada, G. A., Burton, S. P. Ferrare, R., Doherty, S. J., Zuidema, P. (2020). Modeling the smoky troposphere of the southeast Atlantic: A comparison to ORACLES airborne observations from September of 2016. *Atmospheric Chemistry and Physics*, *20*(19), 11491–11526. doi: 10.5194/acp-20-11491-2020

Shulman, M. L., Jacobson, M. C., Carlson, R. J., Synovec, R. E., & Young, T. E. (1996, Feb). Dissolution behavior and surface tension effects of organic compounds in nucleating cloud droplets. *Geophysical Research Letters*, *23*(3), 277–280. doi: 10.1029/95GL03810

Small, J. D., Chuang, P. Y., Feingold, G., & Jiang, H. (2009). Can aerosol decrease cloud lifetime? *Geophysical Research Letters*, *36*(L16806).

Smith, C., Kramer, R., Myhre, G., Alterskjær, K., Collins, W., Sima, A., et al. (2020). Effective radiative forcing and adjustments in CMIP6 models. *Atmospheric Chemistry and Physics*, 1–37. doi: 10.5194/acp-2019-1212

Soden, B. J., Held, I. M., Colman, R., Shell, K. M., Kiehl, J. T., & Shields, C. A. (2008, Jan). Quantifying climate feedbacks using radiative kernels. *Journal of Climate*, *21*(14), 3504. doi: 10.1175/2007JCLI2110.1

Sourdeval, O., C.-Labonnote, L., Baran, A. J., Mülmenstädt, J., & Brogniez, G. (2016, Oct). A methodology for simultaneous retrieval of ice and liquid water cloud properties. Part 2: Near-global retrievals and evaluation against A-Train products. *Quarterly Journal of the Royal Meteorological Society*, *142*(701), 3063–3081. doi: 10.1002/qj.2889

Sourdeval, O., C-Labonnote, L., Baran, A. J., & Brogniez, G. (2015). A methodology for simultaneous retrieval of ice and liquid water cloud properties. Part I: Information content and case study. *Quarterly Journal of the Royal Meteorological Society*, *141*(688), 870–882.

Sourdeval, O., Gryspeerdt, E., Krämer, M., Goren, T., Delanoë, J., Afchine, A., et al. (2018, Oct). Ice crystal number concentration estimates from lidar–radar satellite remote sensing. Part 1: Method and evaluation. *Atmospheric Chemistry and Physics*, *18*(19), 14327–14350. doi: 10.5194/acp-1 -14327-2018

Spensberger, C., & Sprenger, M. (2018, Jan). Beyond cold and warm: An objective classification for maritime midlatitude fronts. *Quarterly Journal of the Royal Meteorological Society*, *144*(710), 261–277. doi: 10.1002/ qj.3199

Squires, P. (1952, Mar). The growth of cloud drops by condensation. I: General characteristics. *Australian Journal of Scientific Research A Physica! Sciences*, *5*, 59. doi: 10.1071/PH520059

Stevens, B., Bony, S., Farrell, D., Ament, F., Blyth, A., Fairall, C., et al. (2021). EUREC^{4}A. *Earth System Science Data*, *13*(8), 4067–4119. Retrieved from https://essd.copernicus.org/articles/13/4067/2021/ doi: 10.5194/essd-13-4067-2021

Stevens, B., & Feingold, G. (2009, Oct). Untangling aerosol effects on clouds and precipitation in a buffered system. *Nature*, *461*(7264), 607–613. doi: 10.1038/nature08281

Stevens, B., Satoh, M., Auger, L., Biercamp, J., Bretherton, C. S., Chen, X., et al. (2019, Sep). DYAMOND: The DYnamics of the Atmospheric general circulation Modeled On on-hydrostatic Domains. *Progress in Earth and Planetary Science*, *6*(1), 61. doi: 10.1186/s40645-019-0304-z

Stier, P., Schutgens, N. A. J., Bellouin, N., Bian, H., Boucher, O., Chin, M., et al. (2013, Mar). Host model uncertainties in aerosol radiative forcing estimates: Results from the AeroCom

Prescribed intercomparison study. *Atmospheric Chemistry and Physics*, *13*(6), 3245–3270. doi: 10.5194/acp-13-3245-2013

Stjern, C. W., Samset, B. H., Myhre, G., Forster, P. M., Hodnebrog, Ø., Andrews, T., et al. (2017). Rapid adjustments cause weak surface temperature response to increased black carbon concentrations. *Journal of Geophysical Research: Atmospheres*, *122*(21), 11,462–11,481. doi: https://doi.org/10.1002/2017JD027326

Storelvmo, T. (2017, Aug). Aerosol effects on climate via mixed-phase and ice clouds. *Annual Review of Earth and Planetary Sciences*, *45*(1), 199–222. doi: 10.1146/annurev-earth-060115-012240

Storelvmo, T., Boos, W. R., & Herger, . (2014). Cirrus cloud seeding: A climate engineering mechanism with reduced side effects? *Philosophical Transactions of the Royal Society A: Mathematical, Physical and Engineering Sciences*, *372*(2031), 20140116. doi: 10.1098/rsta.2014.0116

Storelvmo, T., & Tan, I. (2015). The Wegener-Bergeron-Findeisen process? Its discovery and vital importance for weather and climate. *Meteorologische Zeitschrift*, *24*(4), 455–461. doi: 10.1127/metz/2015/0626

Sullivan, R. C., Moore, M. J. K., Petters, M. D., Kreidenweis, S. M., Roberts, G. C., & Prather, K. A. (2009, May). Effect of chemical mixing state on the hygroscopicity and cloud nucleation properties of calcium mineral dust particles. *Atmospheric Chemistry and Physics*, *9*(10), 3303–3316. doi: 10.5194/acp-9-3303-2009

Tan, I., Storelvmo, T., & Choi, Y.-S. (2014). Spaceborne lidar observations of the ice-nucleating potential of dust, polluted dust, and smoke aerosols in mixedphase clouds. *Journal of Geophysical Research: Atmospheres*, *119*(11), 6653–6665. doi: 10.1002/2013JD021333

Tao, W.-K., Chen, J.-P., Li, Z., Wang, C., & Zhang, C. (2012). Impact of aerosols on convective clouds and precipitation. *Reviews of Geophysics*, *50*(2). doi: https://doi.org/10.1029/2011RG000369

Tegen, I., & Schepanski, K. (2018). Climate feedback on aerosol emission and atmospheric concentrations. *Current Climate Change Reports*, *4*(1), 1–10.

Terai, C. R., Pritchard, M. S., Blossey, P., & Bretherton, C. S. (2020). The impact of resolving subkilometer processes on aerosol-cloud interactions of low-level clouds in global model simulations. *Journal of Advances in Modeling Earth Systems*, *12*(11), e2020MS002274. doi: 10.1029/2020MS002274

Tessendorf, S. A., French, J. R., Friedrich, K., Geerts, B., Rauber, R. M., Rasmussen, R. M., et al. (2019, Jan). A transformational approach to winter orographic weather modification research: The S OWIE project. *Bulletin of the American Meteorological Society*, *100*(1), 71–92. doi: 10.1175/BAMS-D-17-0152.1

Thornton, J. A., Virts, K. S., Holzworth, R. H., & Mitchell, T. P. (2017). Lightning enhancement over major oceanic shipping lanes. *Geophysical Research Letters*, *44*(17), 9102–9111. doi: 10.1002/2017GL074982

Thouron, O., Brenguier, J.-L., & Burnet, F. (2012, May). Supersaturation calculation in large eddy simulation models for prediction of the droplet number concentration. *Geoscientific Model Development*, *5*(3) 761–772. doi: 10.5194/gmd-5-761-2012

Toll, V., Christensen, M., Gassó, S., & Bellouin, . (2017). Volcano and ship tracks indicate excessive aerosol-induced cloud water increases in a climate model. *Geophysical Research Letters*, *44*(24), 12,492–12,500. doi: 10.1002/2017GL075280

Toll, V., Christensen, M., Quaas, J., & Bellouin, . (2019, Aug). Weak average liquid-cloud-water response to anthropogenic aerosols. *Nature*, *572*(7767), 51–55. doi: 10.1038/s41586-019-1423-9

Tornow, F., Domenech, C., Barker, H. W., Preusker, R., & Fischer, J. (2020, Jul). Using two-stream theory to capture fluctuations of satellite-perceived TOA SW radiances reflected from clouds over ocean. *Atmospheric Measurement Techniques*, *13*(7), 3909–3922. doi: 10.5194/amt-13-3909-2020

Twohy, C. H., Kreidenweis, S. M., Eidhammer, T., Browell, E. V., Heymsfield, A. J., Bansemer, A. R., et al. (2009, Jan). Saharan dust particles nucleate droplets in eastern Atlantic clouds. *Geophysical Research Letters*, *36*(1). doi: 10.1029/2008GL035846

Twomey, S. (1954). The composition of hygroscopic particles in the atmosphere. *Journal of Meteorological*, *11*, 334–338.

Twomey, S. (1959, May). The nuclei of natural cloud formation. Part II: The supersaturation in natural clouds and the variation of cloud droplet concentration. *Geofisica Pura e Applicata*, *43*(1), 243–249. doi: 10.1007/BF01993560

Twomey, S. (1974). Pollution and the planetary albedo. *Atmospheric Environment (1967)*, *8*(12), 125!–1256. doi: https://doi.org/10.1016/0004-6981(74)90004-3

Twomey, S. (1977, Jul). The influence of pollution on the shortwave albedo of clouds. *Journal of the Atmospheric Sciences*, *34*(7), 1149–1152. doi: 10.1175/1520-0469(1977)034⟨1149:TIOPOT⟩2.0.CO·2

Twomey, S. A., Piepgrass, M., & Wolfe, T. L. (1984 ov). An assessment of the impact of pollution on global cloud albedo. *Tellus B*, *36B*(5), 356–366. doi: 10.1111/j.1600-0889.1984.tb00254.x

Vergara-Temprado, J., Miltenberger, A. K., Furtado, K., Grosvenor, D. P., Shipway, B. J., Hill, A. A., et al. (2018, Mar). Strong control of Southern Ocean cloud reflectivity by ice-nucleating particles. *Proceedings of the National Academy of Sciences of the United States of America*, *115*(11), 2687–2692. doi: 10.1073/pnas.1721627115

Vonnegut, B. (1958). Early work on silver iodide smokes for cloud seeding. *Final Report of the Advisory Committee on Weather Control*, *2*, 283–285.

Wang, H., Easter, R. C., Rasch, P. J., Wang, M., Liu, X., Ghan, S. J., et al. (2013, Jun). Sensitivity of remote aerosol distributions to representation of cloud–aerosol interactions in a global climate model. *Geoscientific Model Development*, *6*(3), 765–782. doi: 10.5194/gmd-6-765-2013

Wang, M., Ghan, S., Ovchinnikov, M., Liu, X., Easter, R., Kassianov, E., Morrison, H. (2011). Aerosol indirect effects in a multi-scale aerosol-climate model P L-MMF. *Atmospheric Chemistry and Physics*, *11*(11), 5431–5455. doi: 10.5194/acp-11-5431-2011

Wang, S., Wang, Q., & Feingold, G. (2003, Jan). Turbulence, condensation, and liquid water transport in numerically simulated nonprecipitating stratocumulus clouds. *Journal of the Atmospheric Sciences*, *60*(2) 262–278. doi: 10.1175/1520-0469(2003)060⟨0262:TCALWT⟩2.0.CO;2

Wang, S. C., & Flagan, R. C. (1989, Jan). Scanning electrical mobility spectrometer. *Journal of Aerosol Science*, *20*(8), 1485–1488. doi: 10.1016/0021-8502(89) 90868-9

Wang, Y., Su, H., Jiang, J. H., Xu, F., & Yung, Y. L. (2020). Impact of cloud ice particle size uncertainty in a climate model and implications for future satellite missions. *Journal of Geophysical Research: Atmospheres*, *125*(6), e2019JD032119. doi: https://doi.org/10.1029/2019JD032119

Wang, Y., & Zhang, G. J. (2016, Dec). Global climate impacts of stochastic deep convection parameterization in the CAR-CAM5. *Journal of Advances in Modeling Earth Systems*, *8*(4), 1641–1656. doi: 10.1002/2016MS000756

Watson-Parris, D., Bellouin, ., Deaconu, L. T., Schutgens, N. A. J., Yoshioka, M., Regayre, L. A. et al. (2020, May). Constraining uncertainty in aerosol direct forcing. *Geophysical Research Letters*, *47*(9), e2020GL087141. doi: 10.1029/2020GL087141

Watson-Parris, D., Sutherland, S. A., Christensen, M. W., Eastman, R., & Stier, P. (2021, Feb). A large-scale analysis of pockets of open cells and their radiative impact. *Geophysical Research Letters*, *48*(6), e2020GL092213. doi: 10.1029/2020GL092213

Wegener, A. (1911). *Thermodynamik der atmosphäre*. Leipzig: Verlag von Johann Ambrosius Barth.

Wigley, T. M. L. (1989, Jun). Possible climate change due to SO_2-derived cloud condensation nuclei. *Nature*, *339*(6223), 365–367. doi: 10.1038/339365a0

Wilcox, L. J., Liu, Z., Samset, B. H., Hawkins, E., Lund, M. T., Nordling, K., et al. (2020). Accelerated increases in global and Asian summer monsoon precipitation from future aerosol reductions. *Atmospheric Chemistry and Physics*, *20*(20), 11955–11977. doi: 10.5194/acp-20-11955-2020

Williams, K. D., & Webb, M. J. (2009, Jul). A quantitative performance assessment of cloud regimes in climate models. *Climate Dynamics*, *33*(1), 141–157. doi: 10.1007/s00382-008-0443-1

Williamson, C. J., Kupc, A., Axisa, D., Bilsback, K. R., Bui, T. P., Campuzano-Jost, P., et al. (2019, Oct). A large source of cloud condensation nuclei from new particle formation in the tropics. *Nature*, *574*, 399–403. doi: 10.1038/s41586-019-1638-9

Wilson, C. (1900, Jan). IX. On the comparative efficiency as condensation nuclei of positively and negatively charged ions. *Philosophical Transactions of the Royal Society of London. Series A, Containing Papers of a Mathematical or Physical Character*, *193*, 289–308. doi: 10.1098/rsta.1900.0009

Wood, R. (2012). Stratocumulus clouds. *Monthly Weather Review*, *140*(8), 2373–2423. doi: 10.1175/MWR-D-11-00121.1

Wood, R., Ackerman, T., Rasch, P., & Wanser, K. (2017, Jul). Could geo-engineering research help answer one of the biggest questions in climate science? *Earth's Future*, *5*(7), 659–663. doi: 10.1002/2017EF000601

Wood, R., & Ackerman, T. P. (2013, Dec). Defining success and limits of field experiments to test geoengineering by marine cloud brightening. *Climatic Change*, *121*(3), 459–472. doi: 10.1007/s10584-013-0932-z

Wood, R., & Hartmann, D. L. (2006, May). Spatial variability of liquid water path in marine low cloud: The importance of mesoscale cellular convection. *Journal of Climate*, *19*(9), 1748–1764. doi: 10.1175/jcli3702.1

Wood, R., Leon, D., Lebsock, M., Snider, J., & Clarke, A. D. (2012, Oct). Precipitation driving of droplet concentration variability in marine low clouds. *Journal of Geophysical Research: Atmospheres*, *117*(D19). doi: 10.1029/2012jd018305

Wood, R., Stromberg, I. M., Jonas, P. R., & Mill, C. S. (1997, Aug). Analysis of an air motion system on a light aircraft for boundary layer research. *Journal of Atmospheric and Oceanic Technology*, *14*(4), 960–968. doi: 10.1175/1520-0426(1997) 014⟨0960:AOAAMS⟩2.0.CO;2

Woodcock, A. H. (1953, Oct). Salt nuclei in marine air as a function of altitude and wind force. *Journal of Atmospheric Sciences*, *10*(5), 362–371. doi: 10.1175/1520-0469(1953)010⟨0366: SNIMAA⟩2.0.CO;2

Wu, P., Dong, X., Xi, B., Tian, J., & Ward, D. M. (2020, May). Profiles of MBL cloud and drizzle microphysical properties retrieved from ground-based observations and validated by aircraft in-situ measurements over the Azores. *Journal of Geophysical Research: Atmospheres*, *125*(9). doi: 10.1029/2019JD032205

Yamaguchi, T., Feingold, G., Kazil, J., & McComiskey, A. (2015). Stratocumulus to cumulus transition in the presence of elevated smoke layers. *Geophysical Research Letters*, *42*(23), 10,478–10,485. doi: https://doi.org/10.1002/2015GL066544

Yang, F., McGraw, R., Luke, E. P., Zhang, D., Kollias, P., & Vogelmann, A. M. (2019, Nov). A new approach to estimate supersaturation fluctuations in stratocumulus cloud using ground-based remote-sensing measurements. *Atmospheric Measurement Techniques*, *12*(11), 5817–5828. doi: 10.5194/amt-12-5817-2019

Yang, Q., Easter, R. C., Campuzano-Jost, P., Jimenez, J. L., Fast, J. D., Ghan, S. J., et al. (2015, Aug). Aerosol transport and wet scavenging in deep convective clouds: A case study and model evaluation using a multiple passive tracer analysis approach. *Journal of Geophysical Research: Atmospheres*, *120*(16), 8448–8468. doi: 10.1002/2015JD023647

Yin, Y., Carslaw, K. S., & Feingold, G. (2005). Vertical transport and processing of aerosols in a mixed-phase convective cloud and the feedback on cloud development. *Quarterly Journal of the Royal Meteorological Society*, *131*(605), 221–245. doi: https://doi.org/10.1256/qj.03.186

Yoshioka, M., Regayre, L. A., Pringle, K. J., Johnson, J. S., Mann, G. W., Par-tridge, D. G., et al. (2019). Ensembles of global climate model variants designed for the quantification and constraint of uncertainty in aerosols and their radiative forcing. *Journal of Advances in Modeling Earth Systems*, *11*(11), 3728–3754. doi: https://doi.org/10 .1029/2019MS001628

Yuan, T., Remer, L. A., & Yu, H. (2011). Microphysical, macrophysical and radiative signatures of volcanic aerosols in trade wind cumulus observed by the A-Train. *Atmospheric Chemistry and Physics*, *11*(14), 7119–7132. doi: 10.5194/ acp-11-7119-2011

Zelinka, M. D., Myers, T. A., McCoy, D. T., Po-Chedley, S., Caldwell, P. M., Ceppi, P., et al. (2020, Jan). Causes of higher climate sensitivity in CMIP6 models. *Geophysical Research Letters*, *47*(1), e2019GL085782. doi: 10.1029/2019GL085782

Zerefos, C. S., Tetsis, P., Kazantzidis, A., Amiridis, V., Zerefos, S. C., Luterbacher, J., et al. (2014). Further evidence of important environmental information content in

red-to-green ratios as depicted in paintings by great masters. *Atmospheric Chemistry and Physics*, *14*(6), 2987–3015. doi: 10.5194/acp-14-2987-2014

Zhang, Y., Karamchandani, P., Glotfelty, T., Streets, D. G., Grell, G., enes, A., et al. (2012, Oct). Development and initial application of the global-through-urban weather research and forecasting model with chemistry (GU-WRF/Chem). *Journal of Geophysical Research (Atmospheres)*, *117*(D20), D20206. doi: 10.1029/2012JD017966

Zhang, Z., Song, H., Ma, P. L., Larson, V. E., Wang, M., Dong, X., & Wang, J. (2019). Subgrid variations of the cloud water and droplet number concentration over the tropical ocean: Satellite observations and implications for warm rain simulations in climate models. *Atmospheric Chemistry and Physics*, *19*(2), 1077–1096. doi: 10.5194/acp-19-1077-2019

Zhang, Z., Werner, F., Cho, H. M., Wind G., Platnick, S., Ackerman, A. S., et al. (2016). A framework based on 2-D Taylor expansion for quantifying the impacts of subpixel reflectance variance and covariance on cloud optical thickness and effective radius retrievals based on the bispectral method. *Journal of Geophysical Research: Atmospheres*, *121*(12), 7007–7025. doi: 10.1002/2016JD024837

Zhao, B. Wang, Y., Gu, Y., Liou, K.- ., Jiang, J. H., Fan, J., et al. (2019). Ice nucleation by aerosols from anthropogenic pollution. *Nature Geoscience*, *12*(8), 602–607.

Zheng, G., Wang, Y., Wood, R., Jensen, M. P., Kuang, C., McCoy, I. L., et al. (2021). New particle formation in the remote marine boundary layer. *Nature Communications*, *12*(1). doi: 10.1038/s41467-020-20773-1

Zhou, C., & Penner, J. E. (2014). Aircraft soot indirect effect on large-scale cirrus clouds: Is the indirect forcing by aircraft soot positive or negative? *Journal of Geophysical Research: Atmospheres*, *119*(19), 11,303–11,320. doi: https://doi.org/10.1002/2014JD021914

Zhou, X., Ackerman, A. S., Fridlind, A. M., Wood, R., & Kollias, P. (2017). Impacts of solar-absorbing aerosol layers on the transition of stratocumulus to trade cumulus clouds. *Atmospheric Chemistry and Physics*, *17*(20), 12725–12742. doi: 10.5194/acp-17-12725-2017

Zhu, J., & Penner, J. E. (2020). Radiative forcing of anthropogenic aerosols on cirrus clouds using a hybrid ice nucleation scheme. *Atmospheric Chemistry and Physics*, *20*(13), 7801–7827. doi: 10.5194/acp-20-7801-2020

Zuidema, P. Redemann, J., Haywood, J., Wood, R., Piketh, S., Hipondoka, M., & Formenti, P. (2016, Jul). Smoke and clouds above the southeast Atlantic: Upcoming field campaigns probe absorbing aerosol's impact on climate. *Bulletin of the American Meteorological Society*, *97*(7), 1131–1135. doi: 10.1175/BAMS-D-15-00082.1

Zuidema, P., Sedlacek, A. J., Flynn, C., Springston S., Delgadillo, R., Zhang, J., et al. (2018, May). The Ascension Island boundary layer in the remote southeast Atlantic is often smoky. *Geophysical Research Letters*, *45*(9) 4456–4465. doi: 10.1002/2017GL076926